**Atmospheric
Chemistry
and Physics**

Turbulent exchange and segregation of HO_x radicals and volatile organic compounds above a deciduous forest

R. Dlugi[1], M. Berger[1], M. Zelger[1], A. Hofzumahaus[2], M. Siese[2], F. Holland[2], A. Wisthaler[3], W. Grabmer[3], A. Hansel[3], R. Koppmann[2,4], G. Kramm[5], M. Möllmann-Coers[6], and A. Knaps[6]

[1]Arbeitsgruppe Atmosphärische Prozesse (AGAP), München, Germany
[2]Institut für Chemie und Dynamik der Geosphäre 2 (ICG-2): Troposphäre, Forschungszentrum Jülich, Jülich, Germany
[3]Leopold Franzens – Universität, Institut für Ionenphysik und Angewandte Physik (IAP), Innsbruck, Austria
[4]Fachgruppe Physik, Fachbereich Mathematik und Naturwissenschaften, Bergische Universität Wuppertal,
Wuppertal, Germany
[5]Geophysical Institute, University of Alaska, Fairbanks, USA
[6]Geschäftsbereich Sicherheit, Forschungszentrum Jülich, Jülich, Germany

Abstract. The eddy covariance method was applied for the first time to estimate fluxes of OH and HO_2 together with fluxes of isoprene, the sum of methyl vinyl ketone (MVK) and methacrolein (MACR) and the sum of monoterpenes above a mixed deciduous forest. Highly sensitive measurements of OH and HO_2 were performed by laser induced fluorescence (LIF), and biogenic volatile organic compounds (BVOCs) were measured by Proton-Transfer-Reaction Mass Spectrometry (PTR-MS) at a time resolution of 5 s, each. Wind speed was measured by a sonic anemometer at 10 Hz. The one-day feasibility study was conducted at a total height of 37 m, about 7 m above forest canopy, during the ECHO (Emission and CHemical transformation of biogenic volatile Organic compounds) intensive field study in July 2003. The daytime measurements yielded statistically significant OH fluxes directed downward into the direction of the canopy and HO_2 fluxes mainly upward out of the canopy. This hints towards a significant local chemical sink of OH by reactions with BVOCs, other organic and inorganic compounds and conversion of OH to HO_2 above the canopy. For OH the measured flux is locally balanced by chemical sources and sinks and direct transport of OH plays no important role for the local chemical OH budget at the measurement height, as expected from the short OH lifetime (<1 s). For HO_2 the chemical lifetime (20 s) is in the range of the turbulent transport time for transfer between the top of the canopy and the

measuring point. In this case, the radical balance is significantly influenced by both chemistry and transport processes. In addition, the highly time-resolved trace gas measurements were used to calculate the intensity of segregation of OH and BVOCs, demonstrating that the effective reaction rate of isoprene and OH was slowed down as much as 15% due to inhomogeneous mixing of the reactants. The paper describes the results, the applied methods and provides a detailed analysis of possible systematic errors of the covariance products.

1 Introduction

Biogenic volatile organic compounds (BVOCs) have a significant influence on tropospheric chemistry on local to global scales (e.g. Fuentes et al., 2000; Poisson et al., 2000). BVOCs, including isoprene (C_5H_8) and monoterpenes ($C_{10}H_{16}$), influence the atmospheric oxidation capacity by reaction with hydroxyl radicals (OH), nitrate radicals (NO_3) and ozone (O_3) (e.g. Atkinson and Arey, 2003; Finlayson-Pitts and Pitts, 1986; Seinfeld and Pandis, 1988) and contribute to the formation of secondary chemical products including ozone, oxygenated volatile organic compounds (OVOCs) and secondary organic aerosols (SOA) (e.g. Sanderson et al., 2003; Hallquist et al., 2009). BVOCs contribute also significantly to the carbon budget of the biosphere (e.g. Kesselmeier and Staudt, 1999). For these reasons, their emission from the terrestrial vegetation into the troposphere is of general interest.

The rate of BVOC emissions depends on many variables and is mainly controlled by plant physiological status and meteorological conditions like temperature, solar radiation and humidity (e.g. Guenther et al., 1995, 2006; Kesselmeier and Staudt, 1999). Estimates of the net emission of organic compounds from forests take these variables into account, but are additionally complicated by chemical loss and transformation processes resulting from reactions with OH, NO_3 and O_3 in the mixing-layer type flow regime (ML) near canopy top (denoted by height h_c) as well as inside the canopy atmosphere (CA). The chemistry impact within and above a forest canopy has been investigated in various model studies (Gao et al., 1993; Makar et al., 1999; Stroud et al., 2005; Forkel et al., 2006; Guenther et al., 2006). For example, the isoprene flux, F_{iso}, at h_c was estimated to be reduced by chemical reactions by about 12% (Gao et al., 1993) and up to about 40% (Makar et al., 1999) or even more (Butler et al., 2008) compared to the vertically integrated emission from leaf surfaces. Experimental evidence for significant chemical conversion of BVOCs in forest stands has been reported from several field studies (e.g. Bouvier-Brown et al., 2009; Di Carlo et al., 2004; Karl et al., 2004; Spirig et al., 2005; Holzinger, 2005; Schaub, 2007; Valentini et al., 1997; Zelger et al., 1997). For example, not only fluxes of primary emitted BVOCs, but also of oxidized reaction products could be measured (e.g. Karl et al., 2003, 2004). Recently, Spirig et al. (2005) determined fluxes of the sum of reaction products of isoprene, e.g. methyl vinyl ketone (MVK) and methacrolein (MACR), together with the flux of isoprene above a mixed deciduous forest (near h_c) during the ECHO campaign 2003 (see below). Simultaneously measured ratios of MVK+MACR to isoprene were analyzed by Schaub (2007), who estimated a residence time of about 20 to 30 min for isoprene in the canopy atmosphere. This time is long enough that measurable amounts of chemical products can be formed inside the canopy.

Transport and chemistry in the ML and CA are influenced by nonlocal mixing processes which cause inhomogeneities in scalar fields (e.g. Kaimal and Finnigan, 1994; Katul et al., 1997; Raupach et al., 1996; Wahrhaft, 2000). It should be noted that the effective reaction rate (e.g. of OH with biogenic hydrocarbons) is lower for incompletely mixed reactants than for perfectly mixed constituents. This segregation effect is largest, if the characteristic time scale of turbulent mixing, τ_T, is comparable to the characteristic chemical reaction time scale, τ_{ch} (e.g. Damköhler, 1957; Astarita, 1967; Komori et al., 1991).

Aubrun et al. (2005) physically modelled the complex forest area at the ECHO field site in a wind tunnel. From their studies it is most likely that the assumptions made for the model studies performed by Krol et al. (2000) and Patton et al. (2001) are comparable to the situations at our measuring site. Krol et al. (2000) modelled reactions of hydrocarbons with OH in the atmospheric mixing layer and found that the effective reaction rates can be smaller by up to about 30%,

compared to the well mixed case, by the influence of spatial horizontal heterogeneity of BVOC emission source strength. Patton et al. (2001) studied the influence of intermittent turbulence above and inside a forest canopy by a large-eddy simulation and found a strong vertical dependence of segregation influence from above canopy levels to heights near the soil surface. They calculated effective reaction rates being lower up to 25% inside the canopy and between 1–17% above canopy for the reaction OH + isoprene. From experiments to study emission, chemistry and transport of BVOCs in the atmosphere above forests in Amazonia and Guyana, significant segregation of OH and isoprene is reported (Karl et al., 2007; Butler et al., 2008). Karl et al. (2007) estimated the effect using data of a PTR-MS instrument for isoprene and water vapor as a proxy for OH in a cloud topped boundary layer. According to their work, the relative reduction of the reaction rate constant due to incomplete mixing is 39%±7%. Butler at al. (2008) interpreted their aircraft measurements of OH and isoprene mixing ratios in and above the atmospheric boundary layer above the Guyana rain forest by an influence of segregation with a reduction of the effective reaction rate up to 50%. The quantification of such segregation effects is not only important for estimating net emissions of BVOCs from vegetation, but also for the quantitative understanding of the photochemistry in forested environments. To our knowledge, so far, OH segregation has not been measured close to a BVOC emission source above or in a forest canopy.

OH and HO_2 radicals play a central role in the chemical processing of organic compounds in the atmosphere (e.g. Ehhalt, 1999). OH is the major daytime oxidant which is primarily formed by reaction of water vapor with $O(^1D)$ atoms from ozone photolysis. Other OH sources include photolysis of nitrous acid (HONO) and ozonolysis of alkenes. Hydroperoxy radicals (HO_2) are intermediate products resulting from reactions of BVOCs with OH, and have the ability to recycle OH by reaction with nitrogen monoxide (NO). Relatively few measurements of atmospheric HO_x (OH+HO_2) exist in forest areas. Measurements of OH and HO_2 concentrations were performed above a deciduous forest (Tan et al., 2001) and inside a coniferous forest (Carslaw et al., 2001). While the modelled HO_2 concentrations almost agreed with measured data at the deciduous forest site, the modelled OH concentrations were substantially lower than the measured values in both studies, by a factor of about 2–3 at the deciduous forest site and a factor of two in the coniferous forest. A segregation effect was not considered. It should be noted that the tendency of chemical models to underpredict observed OH at conditions of high VOC (with a strong contribution of isoprene) agrees with those reported by Butler et al. (2008) and Hofzumahaus et al. (2009) at low NO mixing ratios. Di Carlo et al. (2004) interpreted such findings by a missing (not measured) contribution from the reactions of ozone with unsaturated hydrocarbons with a significant net yield of OH (e.g. Kroll et al., 2001).

In order to close some gaps in knowledge related to the emission of BVOCs and the photochemistry in forests, the field campaign ECHO 2003 was performed in a mixed deciduous forest at Forschungszentrum Jülich, Germany, in summer 2003. Some objectives of the ECHO project were

1. to improve the understanding of the interactions between emissions, deposition, chemical transformation and transport on the scale of a forest stand and the mesoscale,

2. to find out the conditions for which a stand acts as a chemical reactor with and without the influence of segregation,

3. to improve the understanding of nitrogen cycling in the soil-vegetation-atmosphere system including the role and behaviour of reactive compounds like NO, NO$_2$, or HONO, and

4. to study the chemical cycles of radicals (OH, HO$_2$, NO$_3$) in and above the forest atmosphere.

ECHO was also designed to study the capability of a special instrumental arrangement to determine local turbulent quantities like covariances (fluxes) of OH, HO$_2$, isoprene, the sum of the monoterpenes and the reaction products MVK and MACR under field conditions. The analysis of the results includes also the determination of the influence of chemical reactions and fluxes on budgets of radicals. In this context, the influence of segregation is examined. Measurements of vertical profiles of HO$_x$ were performed by laser-induced fluorescence (LIF) in parallel to measurements of mixing ratios and fluxes of various reactive trace gases (e.g. NO, NO$_2$, O$_3$, HCHO, HONO), BVOCs (e.g. methanol, acetaldehyde, isoprene, methacrolein, methyl vinyl ketone, monoterpenes), photolysis frequencies and micrometeorological parameters (Amman et al., 2004; Aubrun et al., 2005; Spirig et al., 2005; Kleffmann et al., 2005; Bohn, 2006a, b; Schaub, 2007). The results, for example, showed a decreasing mean OH concentration from canopy top (h_c=30 m) to the ground (A. Hofzumahaus, personal communication, 2010) in parallel to the decreasing mean actinic flux and ozone photolysis frequency $J(\mathrm{O^1D})$ inside the canopy (Bohn, 2006a, b). In addition, nitrous acid was found to be a major source of OH in the ML above that forest (Kleffmann et al., 2005).

During the ECHO campaign, it became obvious that the concentrations of isoprene, MVK + MACR, monoterpenes, and HO$_x$ exhibited fast and strong fluctuations on a time scale of seconds, which were possibly caused by turbulent transport, vertical concentration gradients and incomplete mixing of the reactive components in ambient air. In order to quantify these possible effects, a one-day feasibility study was performed directly above the forest canopy, using LIF and proton-transfer-reaction mass spectrometry (PRT-MS) concurrently at close distance to measure HO$_x$ and BVOCs, respectively, at a high time resolution. For this purpose, the

operation of LIF was adapted to the time resolution (5 s) of the PTR-MS instrument. In addition, meteorological parameter (radiation, humidity, temperature, 3-dimensional wind, photolysis frequencies) were recorded in parallel. In the present paper, the experimental setup is described (Sect. 3) and the time series of the observed trace gases are analyzed, starting from the local mass balance equation of the reactive components (e.g. Businger, 1986; Lenschow, 1995) (Sect. 2). The covariance method is used to estimate, for the first time, turbulent fluxes for radicals, BVOCs, reaction products (MVK + MACR), and sensible heat, together (Sect. 5). Furthermore, the influence of inhomogeneous mixing (segregation) on the reaction rate of OH with isoprene and monoterpenes is quantified.

2 Flux measurements

2.1 Basic concept

The measurement procedures are derived from the local mass balance equation for the ith constituent (e.g. de Groot and Mazur, 1969; Businger, 1986; Kramm and Meixner, 2000; Kramm et al., 2008) per unit volume of air. For a macroscopic flow, the balance equation reads

$$\frac{\partial \rho_i}{\partial t} + \nabla \cdot (\rho_i \boldsymbol{v} + \boldsymbol{J}_i) = Q_i - S_i. \tag{1}$$

Here, the term $\partial \rho_i / \partial t$ is the local derivative of the partial density ρ_i with respect to time, $\boldsymbol{v}$ is the vector of the barycentric velocity (here the wind vector, see Eq. (A4) in Appendix A), $\boldsymbol{J}_i = \rho_i (\boldsymbol{v}_i - \boldsymbol{v})$ is the diffusion flux density (hereafter, a flux density is simply denoted as a flux), $\boldsymbol{v}_i$ is the individual velocity, and ∇ is the nabla or del operator expressed, for instance, in Cartesian coordinates by $\nabla = \boldsymbol{i} \frac{\partial}{\partial x} + \boldsymbol{j} \frac{\partial}{\partial y} + \boldsymbol{k} \frac{\partial}{\partial z}$, where $\boldsymbol{i}$, $\boldsymbol{j}$ and $\boldsymbol{k}$ are the unit vectors in east (x), north (y), and vertical (z) direction, respectively. Furthermore, Q_i represents the sources and S_i the sinks of matter in the fluid due to chemical reactions and/or phase transition processes. Moreover, the quantities $\rho_i \boldsymbol{v}$ and $\boldsymbol{J}_i$ are frequently called the convective and non-convective flux of matter, respectively. The further discussion in Appendix A summarizes the essential procedure to derive a simplified form of Eq. (1) for turbulent flows. Thus, applying the Reynolds' averaging calculus to Eq. (1) yields

$$\frac{\partial \overline{\rho_i}}{\partial t} + \nabla \cdot \left(\overline{\rho_i} \, \overline{\boldsymbol{v}} + \overline{\rho_i' \boldsymbol{v}'} + \overline{\boldsymbol{J}_i} \right) = \overline{Q_i} - \overline{S_i}. \tag{2}$$

It is denoted as the balance equation for the 1st moment (or 1st order balance equation). Here, $\overline{\rho_i' \boldsymbol{v}'}$ is the turbulent flux, also called the eddy flux. It is a non-convective flux, too.

For the stationary conditions of an incompressible flow (see Appendix A) and the further assumption that the fields of the wind velocity and the partial densities of the atmospheric

constituents are horizontally homogeneously distributed, we will obtain

$$\frac{\partial}{\partial z}\left(\overline{\rho_i}\,\overline{w}+\overline{\rho_i'w'}+\overline{J_{i,z}}\right)=\overline{Q_i}-\overline{S_i} \tag{3}$$

and

$$\frac{\partial \overline{w}}{\partial z}=0, \tag{4}$$

where w is the vertical component of the wind vector. From Eq. (4) we may infer that $\overline{w}$ is constant with height. Since at any rigid surface $\overline{w}$ is equal to zero, we may state that $\overline{w}$ is generally equal to zero under the conditions that the fluid is incompressible and horizontally homogeneous. Sun (2007) discussed some of these limitations for canopy flow. Under these premises, the vertical contribution to the flux divergence is compensated by the sources and sinks due to chemical reactions and/or phase transition processes. In a fully turbulent flow, the molecular diffusion flux of a gaseous entity can be neglected because $\left|\overline{\rho_i'w'}\right|\gg\left|\overline{J_{i,z}}\right|$. Integrating Eq. (3) over a certain height interval, $[z_f,z_R]$, where z_f is a reference height for the foliage ($z_f=0$ for bare soil), and z_R is a reference height above the canopy at which the eddy flux measurements are performed (e.g. $z_R=1.23h_c$, as in the present work), yields

$$\left(\overline{\rho_i'w'}+\overline{J_{i,z}}\right)_{z=z_f}=\overline{\rho_i'w'}\Big|_{z=z_R}-\int_{z_f}^{z_R}\left(\overline{Q_i}-\overline{S_i}\right)dz. \tag{5}$$

This equation describes the way in which fluxes related to the emission or uptake of gaseous matter at $z=z_f$ can be related to the measured eddy flux $F_i=\overline{\rho_i'w'}$ at $z=z_R$ of this entity under the influence of (chemical) sources (Q$_i$) or sinks (S$_i$) in the atmospheric layer $\Delta z=z_R-z_f$.

Note, that in the case of horizontally inhomogeneous conditions, all other terms like horizontal or vertical advection in Eq. (2) will also contribute to the local mass balance. In addition, near sources of reactive BVOCs, not only turbulent or convective mixing, but also an inhomogeneous distribution of sources at surfaces (which appear in the boundary conditions in Eqs. 2 or 5) can influence the net divergence in the volume of the atmosphere (e.g. Krol et al., 2000).

2.2 Turbulent transport and chemical reactions

A significant flux divergence can occur in Eq. (5), if the chemical reaction time scale τ_{ch} is comparable to the time scale τ_T for vertical turbulent transport over the distance z_R from the measuring point to the Earth surface ($z_f=0$) or another point in the canopy ($z_f>0$), where emission or deposition happens (e.g. Ebel et al., 2007; Dlugi, 1993; Fitzjarrald and Lenschow, 1983; Komori et al., 1991; Kramm and Dlugi, 1994; Kramm et al., 1995; Stockwell, 1995; Vila-Guerau de Arellano et al., 1993; Zelger et al., 1997). The relation $Da=\tau_T/\tau_{ch}$ is called the Damköhler number (e.g.

Vila-Guerau de Arellano et al., 1995). For $\tau_T\ll\tau_{ch}$ the chemical constituents can be considered to be inert like a tracer and the integral term in Eq. (5) vanishes. However, for $\tau_T\gg\tau_{ch}$ the species vary as if driven by chemical kinetics or to be in chemical equilibrium. Stockwell (1995) analysed reactions of a gas-phase chemical mechanism and found the reactions of OH (e.g. OH+NO$_2$, OH+CO, OH+BVOC) and the reaction HO$_2$+NO to be diffusion limited under typical turbulent atmospheric conditions, or between diffusion limitation ($\tau_T\approx\tau_{ch}$) and kinetic regime ($\tau_T\gg\tau_{ch}$) for vertical transport under near neutral to unstable conditions. This result agrees with findings from model studies by Krol et al. (2000), Verver et al. (2000) and Ebel et al. (2007). As a consequence, the covariances between the vertical velocity component and OH or HO$_2$, and also reactive biogenic hydrocarbons like isoprene should be considered in terms of sources and sinks in Eq. (5).

Incomplete mixing of two reactants ρ_i, ρ_j (e.g. OH, isoprene) inside a volume of air results in a reduced net reaction rate $R_{\rho_i\rho_j}$

$$R_{\rho_i\rho_j}=k\,\overline{\rho_i}\cdot\overline{\rho_j}\left[1+\left(\frac{\overline{\rho_i'\rho_j'}}{\overline{\rho_i}\cdot\overline{\rho_j}}\right)\right] \tag{6}$$

compared to the homogeneously mixed case with $R_{\rho_i\rho_j}=k\overline{\rho_i}\cdot\overline{\rho_j}$. According to the averaging procedure explained in Appendix A (see also Sect. 2.3), the overbars describe the time averaged quantities, and $\overline{\rho_i'\rho_j'}$ the covariance between ρ_i and ρ_j (e.g. Vinuesa and Vila-Guerau de Arellano, 2005). The quotient in brackets ($\overline{\rho_i'\rho_j'}/\overline{\rho_i}\cdot\overline{\rho_j}$), the intensity of segregation I_s, is estimated within the two limits $I_s=0$ for ideal (homogeneous) mixing and $I_s=-1$ for unmixed conditions (e.g. Komori et al., 1991; Wahrhaft, 2000). Note, that the intensity of segregation can also be positive if the species are initially premixed (e.g. Toor, 1969) and if reactants are transported together. The ratio of reactant concentrations is also important, if the reactions and the magnitude of segregation intensities are considered.

Fluxes of OH, HO$_2$ and isoprene as well as its reaction products MVK + MACR are presented in Sect. 5.2. In addition, and for comparison with results of Spirig et al. (2005), the flux of the sum of monoterpenes is given. The intensity of segregation I_s is estimated for the sink reactions of OH with isoprene and the sum of monoterpenes in Sect. 5.3.

2.3 The covariance method

The covariance method determines terms like $\overline{w'\rho_i'}$ in Eqs. (2) and (5), or $\overline{\rho_i'\rho_j'}$ in Eq. (6). As discussed in Appendix A, the fluctuations $\varphi'(x)$ of quantity $\varphi(x)$ (wind component or partial density) from a mean $\overline{\varphi}(x)$ at a point with the coordinate x are given by $\varphi'(x)=\varphi(x)-\overline{\varphi}(x)$. The mean value $\overline{\varphi}(x)$ is obtained by averaging $\varphi(x)$ over a sufficiently long time period (e.g. Lippmann, 1952; Stull, 1988).
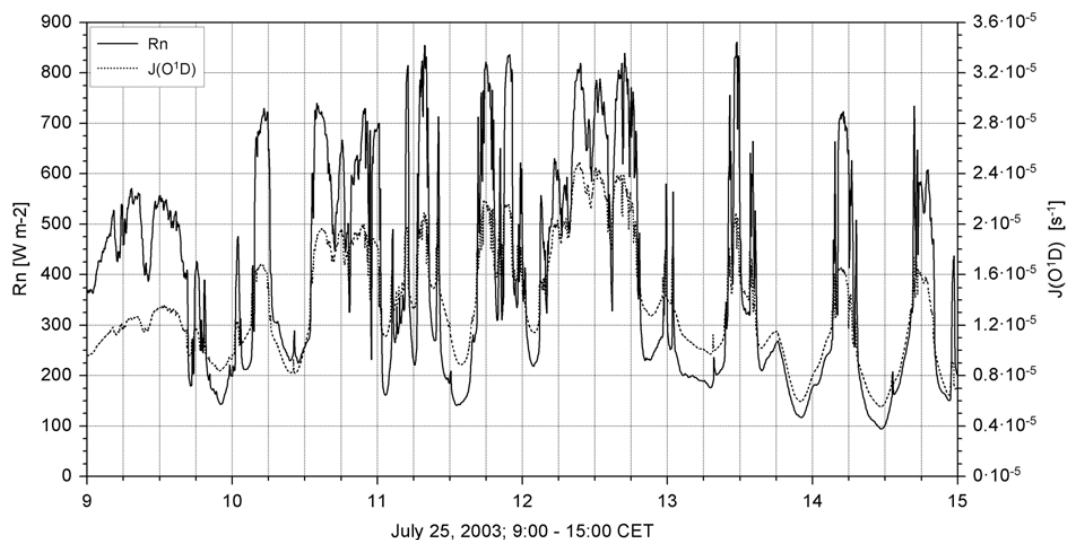
Fig. 1. Net radiation Rn (Wm^{-2}) and $J(O^1D)$ – photolysis frequency (s^{-1}) for 25 July 2003, 09:00–15:00 CET above canopy.

Therefore, the covariance for equidistant values of w and ρ_i (i.e. with constant time step Δt) is given by Eq. (7)

$$\overline{w'\rho'_i} = \frac{1}{N}\sum_{k=1}^{N}(w_k - \overline{w})(\rho_{i,k} - \overline{\rho_i}) \tag{7}$$

where N is the number of data points separated by Δt in the integration interval $\Delta = N \cdot \Delta t$ with the common range $600\,s \leq \Delta \leq 3000\,s$ (e.g. Lenschow and Hicks, 1989; Beier and Weber, 1992). The coordinate system is given according to the definition of a flux as a quantity transported normal to the Earth surface (e.g. Stull, 1988; Sun, 2007) by the vertical axis parallel to the geopotential and the other axis with a right handed geographic coordinate system ($x = W - E$ component, y = $S - N$ component). In terms of Sun (2007), these are the local Earth coordinates (LEC).

3 Experimental

3.1 General description

The ECHO 2003 intensive field campaign was performed from 17 June to 6 August. Three towers were installed in a mixed deciduous forest with dominating tree species beech, birch, oak and ash, and a mean canopy height h_c=30 m. The vertically integrated one-sided leaf area index in a radius of 50 m around the main tower varied between 5.5 and 5.8. The main tower and the west tower were aligned parallel to the main wind direction (Schaub, 2007). This allowed us to investigate the influence of the spatial distribution of BVOC-sources (isoprene, monoterpenes) on measured fluxes (e.g. Spirig et al., 2005). The flux measurements reported in the present paper were obtained on 25 July, 09:00 to 15:00 CET on the main tower. The main tower with a height of 41 m, and

the upper measuring platform at 36 m, was equipped with 9 sonic anemometers / thermometers (METEK, instrument type: USA-1; time resolution 10 Hz) between 2 m and 41 m, and 8 psychrometers (dry and wet bulb temperatures) at the same heights except 41 m. Radiation quantities and photolysis frequencies were obtained by radiometers directly above the canopy (h_c=30 m) (Bohn et al., 2004, 2006a, b). OH and HO_2 radical concentrations were measured by LIF (Holland et al., 1995, 2003) on a vertically movable platform, which was positioned above the canopy, with the inlet at 37 m height (Kleffmann et al., 2005). A PTR-MS instrument for measurement of isoprene, monoterpenes, MVK and MACR was installed at the ground, using a sampling line to collect air at the height of the ultrasonic anemometer (Ammann et al., 2004; Spirig et al., 2005). The distances of the inlets of the PTR-MS and LIF instruments from the ultrasonic-anemometer measuring volume were 0.45 m and 0.6 m, respectively. This spatial arrangement requires corrections to the calculated fluxes as is outlined below. For all aspects identical to the procedures as applied by Spirig et al. (2005), we refer to their work. Aspects which we handled in a different way are described in more detail in the following. The mean meteorological conditions above the canopy are given in Figs. 1–3 together with the friction velocity as a measure of turbulence.

3.2 Operation of PTR-MS instrument

The principle of operation of the PTR-MS follows the procedures as given by Ammann et al. (2004) and Spirig et al. (2005). Air was pulled through an inlet of a tube down to the ground where the PTR-MS was installed in a field laboratory-container. The ion masses (m) at $m69$ (isoprene), $m71$ (sum of MACR and MVK) and at $m137$ (and

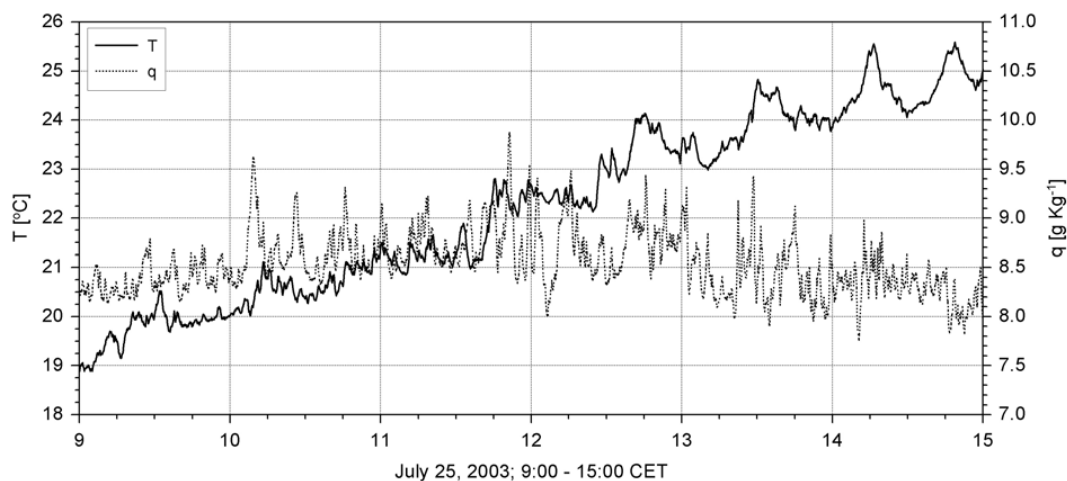**Fig. 2.** Air temperature T (°C) and specific humidity q (g_{H_2O}/kg_{Air}) from psychrometer at 37 m height for 25 July 2003, 09:00–15:00 CET.
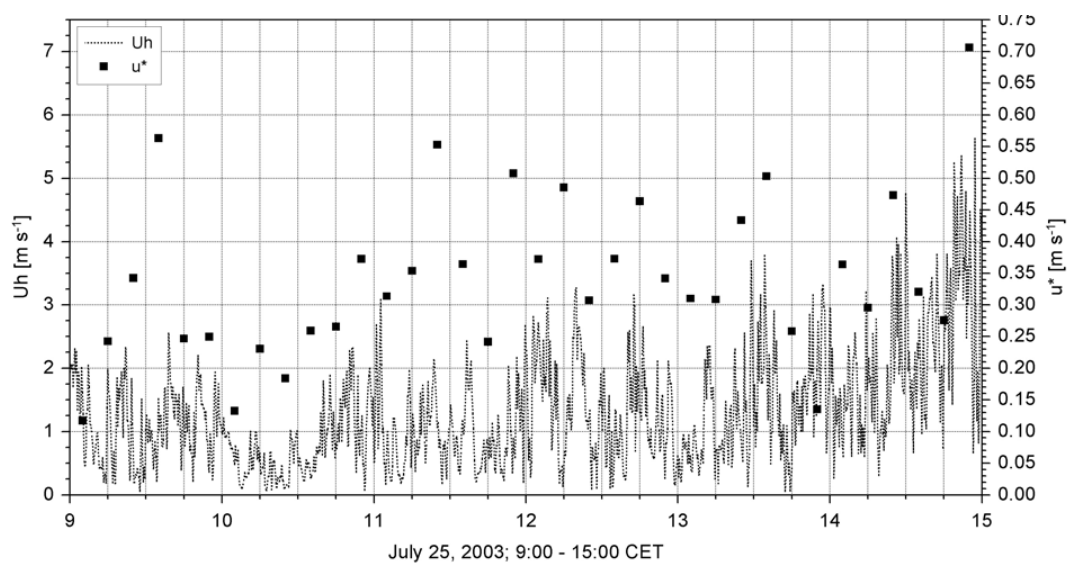

Fig. 3. Horizontal wind velocity Uh (ms^{-1}) and friction velocity (10 min mean) $u*$ (ms^{-1}) at 37 m height for 25 July 2003, 09:00–15:00 CET.

$m81$) (sum of monoterpenes) together with $m21$ (H_3O-18^+) were recorded in an alternating cycle. The measuring cycle is, therefore, comparable to the cycle given by Spirig et al. (2005) in their Fig. 2. The single ion masses are recorded at 0.2 Hz different from Spirig et al. (2005) who recorded at about 0.3 Hz. The dwell times are 0.1 s for primary ions and 0.75 s for the other masses, somewhat larger than the 0.5 s by Spirig et al. (2005) in their Fig. 2. This modification enhances the detection limit by about 23%. For calibration during the complete campaign, gas standards for methanol, ethanol, acetone, acetaldehyde, isoprene and α-pinene from Apel-Riemer, Environmental Inc., Denver, CO, USA were applied. The detection limits (S/N=2) on 25 July 2003 were 42 pptv ($m69$), 38 pptv ($m71$), and 70 pptv ($m137$). The zero point was determined every hour. Other operational parame-

ters were fixed as given by Spirig et al. (2005) in their Table 1 for the main tower also with a total residence time of the sample gas from the inlet tube (at 37 m height) to the drift tube of the PTR-MS at ground level of about 1 s.

3.3 Operation of LIF instrument

The LIF instrument of Forschungszentrum Jülich was a newly built instrument based on the well established concept used previously by the same group (Holland et al., 1995, 2003). The new instrument was designed to be smaller and more light-weight than the previous instrument, making the instrument suitable for tower based application (e.g. Kleffmann et al., 2005). The radicals are sampled by expansion of ambient air through an inlet nozzle into a low pressure

Table 1. Mean percentage underestimation of fluxes for different compounds. In addition the minimum and maximum values for the measuring period 09:00–15:00 CET (25 July 2003) are given. The calculation (Eq. 8) is for $\tau_F = 2$ s.

Compound	Mean (%)	Minimum (%)	Maximum (%)
OH	-37	-33	-42
HO$_2$	-31	-26	-34
Isoprene	-23	-20	-29
Monoterpenes	-33	-28	-39
MVK + MACR	-35	-32	-40

Fig. 4. On (P) and off (U) resonance signals (cts/Vs) for OH (upper panel) and HO$_x$ (lower panel) measured by LIF on 25 July 2003 at 37 m height above ground.

chamber, where OH is detected by LIF at 308 nm. HO$_2$ radicals are monitored in a separate detection chamber, in which HO$_2$ is first chemically converted to OH by reaction with NO, followed by LIF detection of OH. The OH fluorescence is excited by a pulsed narrow-bandwidth UV laser system (DPSS Photonics DS20-532; dye laser LAS Intradye) at a repetition rate of 8.5 kHz and is detected by gated photon-counting after each laser pulse. The laser can be tuned on- and off-resonance to distinguish the OH fluorescence signal from non-resonant background signals (Hofzumahaus et al., 1996). Calibration is performed by known amounts of OH radicals which are generated by photolysis of water vapor at 185 nm (Holland et al., 2003).

The LIF instrument signals were obtained in the following way. The on-resonance signals contain contributions from (1) the laser-power dependent OH fluorescence, (2) laser dependent straylight, (3) a negligible dark signal of the fluorescence detector, (4) scattered solar radiation entering the entrance nozzle, and (5) a contribution from an ozone interference equivalent to the signal of 3×10^5 OH cm^{-3} per 50 ppbv O$_3$. The signal components (1)–(5) for on-resonance are detected in a time window of 500 ns after each laser pulse. The signal contributions (3) and (4) are independent of the laser pulse and are detected with a time delay of 25 µs in a second time window of 25 µs. The difference from both time windows (normalized and projected to the 500 ns window) is the laser dependent signal (cts) being corrected for the influence of scattered sunlight. It is then normalized to the voltage signal (V) of a UV sensitive photodiode which monitors the laser power. The normalized signal is integrated over successive laser pulses for a time period of seconds to improve the signal-to-noise ratio.

The off-resonance signals contain the background contributions (see above) (2)–(4) and are treated in the same way as on-resonance signals, in order to correct for solar background and possible laser-power variations. The difference between the normalized on- and off-resonance signals (Fig. 4) is only caused by fluorescence of the radicals and is transformed to concentrations by calibration (Fig. 5). Normally, the LIF in-
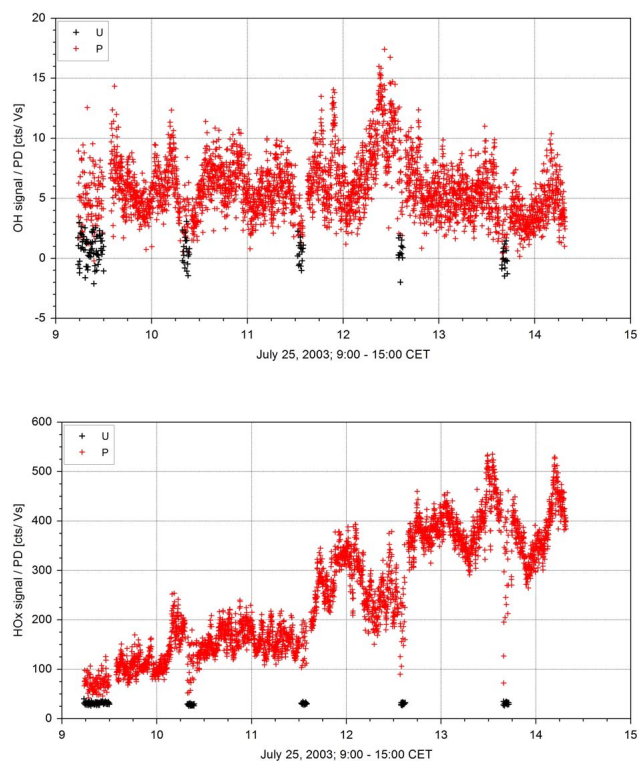
strument is operated in an alternating on- and off-resonance mode with equal integration times, leading to a typical detection limit (S/N=2) of about 5×10^5 OH cm^{-3} for 30 s on- and off-resonance each. For the flux measurements on 25 July, however, each on-resonance period lasted for nearly one hour during which the normalized signals (cts/V) were integrated over 3 s with a total time step of 5 s, leading to a signal collection frequency of 0.20 Hz. After each on-resonance period, the background signal and laser wavelength stability were controlled. For this purpose the complete OH line profile and the off-resonance background were scanned repeatedly (3–4 times) in about 6–7 min, before a new on-resonance period was started. Therefore the resulting time series of OH and HO$_2$ concentrations (Fig. 5) and of second order moments in the following figures exhibit gaps during the time intervals when the calibration procedures were performed.

Measurements of HO$_x$ were obtained during the following time blocks: 09:34–10:18, 10:25–11:30, 11:37–12:33, 12:39–13:38, 13:44–14:19 CET. Figure 4 shows the time series of sunlight-corrected and normalized on- and off-resonance signals (cts/Vs) with the photodiode signal in the range of 2–3 V. The OH signals are between about 1–15 cts/Vs with a background mean of 0.63 cts/Vs (standard deviation = 1.1 cts/Vs). The HO$_2$ on-resonance signals reach maximum values of about 550 cts/Vs with a mean
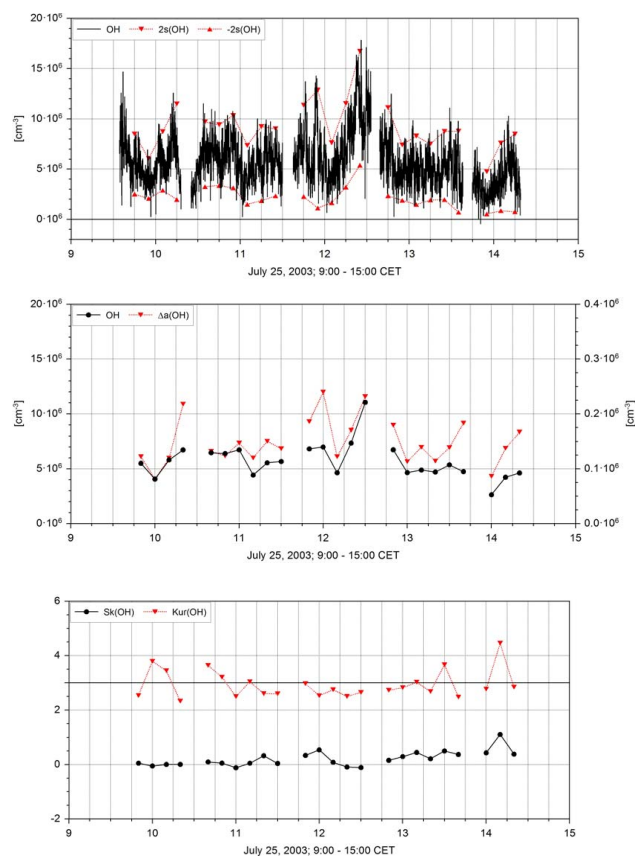
Fig. 5a. Concentration of OH (cm^{-3}) with the $\pm 2\sigma$-limits, the mean value, the standard error Δa (right ordinate), the skewness Sk and the kurtosis Kur, measured at 37 m height by LIF on 25 July 2003, 09:00–15:00 CET.
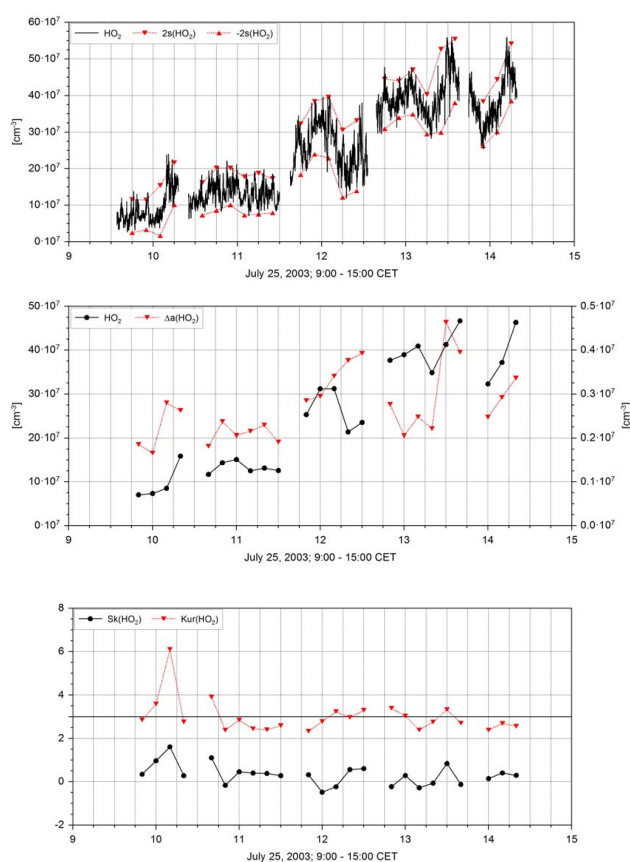
Fig. 5b. Concentration of HO$_2$ (cm^{-3}) with the $\pm 2\sigma$-limits, the mean value, the standard error Δa (right ordinate), the skewness Sk and the kurtosis Kur, measured at 37 m height by LIF on 25 July 2003, 09:00–15:00 CET.

background of 31 cts/Vs (standard deviation = 2.5 cts/Vs). The resulting detection limits (S/N=2) for the OH and HO$_2$ data in Fig. 5 are 3×10^6 cm^{-3} and 8×10^6 cm^{-3}, respectively.

A statistical Z-test (Sachs and Hedderich, 2006) is applied to both data sets to estimate if the variability of the signals (Figs. 4 and 5) is influenced by the precision of measurements. For this purpose the deviations of signals from their mean of consecutive 10 min intervals are considered for a confidence level of α=0.05 (e.g. there is only a chance of rejecting the null hypothesis by 5%). For HO$_2$ the observed variability for the whole time period from 09:00–15:00 CET appears to be mainly real and not influenced by noise. For OH only about one third of the intervals fulfil this criteria with α=0.05. For α=0.15 in 88% of the 10 min-intervals the variability of the signals appears to be real and not caused by the precision of the measurements. These criteria are more restrictive than the determination of the standard error Δa (Fig. 5) which shows that Δa(OH) and Δa(HO$_2$) are well below 10% of their specific mean concentrations. Therefore one should be aware that for the further analysis and dis-

cussion, the resulting HO$_2$ fluxes can be considered to be quantitative, while part of the calculated OH fluxes is still influenced by measurement precision.

For the consideration of segregation it is important to note that a time resolution of 0.2 Hz was chosen, which allowed to apply the same procedures of time series analysis to the data from LIF and PTR-MS instruments and to estimate I_s according to Eq. (6).

3.4 Operation of sonic anemometer

The METEK USA-1 sensor at 37 m height was installed as near as possible to the inlets of the PTR-MS and LIF instruments (0.45 m away from the PTR-MS and 0.6 m away from the LIF inlet). The raw data also contain the exact time stamp, therefore, even small delays in each individual signal could be corrected (Sect. 3.5). The three wind vector components (u, v, w) and the sonic temperature (T_s) were recorded at 10 Hz and post processed together with the data from PTR-MS and LIF. A 3-D sensor correction based on detailed measurements in a wind tunnel of the Meteorological

Institute, University Hamburg, Germany was applied to correct wind vector components raw data for the influence of flow distortion. The influence of this correction for the wind vector components $\boldsymbol{u}$ and $\boldsymbol{v}$ is below 1.5%, but up to 18% for the vertical wind component $\boldsymbol{w}$. Before the application of this correction, the inclination of the axis of each sonic against the geopotential is corrected to better than 0.5° by use of inclinometer data, which is a prerequisite to apply LEC for analysis of turbulence signals (Beier and Weber, 1992; Foken et al., 1995; Sun, 2007).

3.5 Application of the covariance method

Every turbulent time series of wind vector components, temperature, humidity and trace substances show time dependent trends of their means over each integration interval Δ, which have to be eliminated to calculate covariances according to Eqs. (5)–(7). Thus, a low frequency instationarity is separated from a higher-frequency turbulence. In our analysis, the trend correction for 1 min up to 10 min data is performed by a cubic polynomial, while for the 30 min data a symmetric linear Savitzki-Golay low pass filter signal (Press et al., 1991) is subtracted from the initial data set. This net signal is added to the arithmetic mean. This procedure minimizes the resulting residuum even better than linear detrending, while the mean value is conserved. A corresponding test for stationarity with consecutive 2 min samples within Δ=10 min and 5 min samples within Δ=30 min as described by Foken et al. (1995) shows that all covariances fulfilled a criterion $0.8 < (\overline{w'\rho'_i})_{2\min}/(\overline{w'\rho'_i})_{10\min} < 1.2$ for stationarity. This is even stronger than the 30% criterion for Δ=30 min which is often applied (e.g. Spirig et al., 2005; Farmer et al., 2006).

The calculation of turbulent and micrometeorological mean quantities is performed in the following way. After applying the trend correction, the first to fourth moments were calculated for fixed time intervals of 1min, 2 min, 5 min, 10 min, and 30 min. The resulting covariances (fluxes) are given by Eq. (7). All moments and related quantities like turbulence intensities, wind vector, friction velocity u_* or Monin-Obukhov length L_* were calculated in the LEC (Sect. 2.3) and the so-called natural coordinate system (y_n-axis orthogonal to the x_n-axis; y_n-axis parallel to the Earth surface; z_n-axis orthogonal on the x_n–y_n plane). The sensible heat flux is obtained by calibration of T_s against the data obtained from ventilated psychrometers and the application of a procedure as described by Schotanus et al. (1983). An ogive analysis (Oncley, 1989; Beier and Weber, 1992) was added as a quality test for the convergence of the covariance function for each time interval to compare also with data obtained by Spirig et al. (2005). Their spectral correction to the time series to introduce contributions from higher frequencies above 0.20 Hz to fluxes $(\overline{w'\rho'_i})$ of trace substances is not applied in our analysis. Instead flux sampling errors related to the separation of measuring volumes of sensors, their response time and the length of the sampling interval Δ were estimated as discussed in the following and in Sect. 5.2.

In general, signals from the sonic anemometer and gas analyzers like the LIF or PTR-MS instrument are not in coincidence although they were registered with computer systems synchronized by one clock. The time shift relative to the time steps of the sonic anemometer are caused by the time an air parcel needs to move from the measuring volume of the sonic anemometer to the gas analyzer inlets at 37m height (see Sect. 3.1), and in the case of the PTR-MS, the additional transport time of the air sample through tubing to the PTR-MS instrument at ground level. To correct for these time shifts, the covariance between w and ρ_i is calculated versus lag time between w and ρ_i according to Eq. (7). The maximum $(\overline{w'\rho'_i})_{\max}$ of the covariances is taken as the eddy correlation flux in each time interval Δ and for each channel of the instruments as performed also by Beier and Weber (1992), Oncley (1989), Spirig et al. (2005) and Farmer et al. (2006).

The spatial separation of a chemical sensor inlet from the measuring volume of the sonic anemometer causes a flux reduction at the high frequency part of the turbulence spectrum (Moore, 1986). This is most pronounced for frequencies $f > 0.2$ Hz, the limits given by the conditions to run the PTR-MS and the LIF. Using the spectral transfer function of Moore (1986), a maximum loss of 13% for $\overline{w'\rho'}$ compared to instruments which sample from the same volume and with 10 Hz is estimated independently of the specific characteristics of the instruments. As discussed by Spirig et al. (2005), for the ECHO site the long sampling tube also contributes to the damping of amplitudes for frequencies larger than about 1.5 Hz.

In 2003, both chemical sensors (PTR-MS, LIF) had characteristic response times τ_r with respect to a sudden stepwise increase of concentrations at the inlet of τ_r=0.3 s and $\tau_r \leq 0.01$ s, respectively. Horst (1997) showed that the knowledge of the frequency f_m, taken at the maximum of the frequency-multiplied cospectrum, and τ_r are sufficient to estimate the reduction of the measured flux F_i compared to the true flux F_t measured by an ideal instrument with τ_r=0, and resulting in $F_i/F_t < 1$. Applying this method with $f_m \approx 0.018$ Hz and the maximum response times τ_r=0.3 s (PTR-MS) and τ_r=0.01 s (LIF), the fractions $F_i/F_t \approx 0.95$ for the fluxes of BVOCs and $F_i/F_t \approx 1.0$ for the fluxes of HO$_2$ or OH are estimated. These fractions agree with data obtained by Farmer et al. (2006) for their determination of fluxes of reactive nitrogen compounds with thermal-dissociation laser induced fluorescence (TD-LIF).

In general, the sampling interval Δ of 10 min is not long enough to capture all contributions to the covariance from all frequencies. In addition, both chemical sensors are limited to signals with frequencies below 0.20 Hz. This limitation of the sampling interval Δ causes an increasing fractional flux sampling error, which can be estimated by the quotient of the

variance σ_F and the flux F_i. It can be expressed by Eq. (8) as given by Lenschow (1995):

$$\frac{\sigma_F(T)}{|F_i|} = \left(\frac{2\tau_F}{T}\right)^{1/2} \left(\frac{1+r_{wc}^2}{r_{wc}^2}\right)^{1/2}. \tag{8}$$

There, τ_F is the integral timescale of the flux estimated from the spectra of F_i by Lenschow et al. (1994) or the autocorrelation function by Kaimal and Finnigan (1994), and r_{wc} is the correlation coefficient between w and ρ_i for the adjusted time series with $F_i = (\overline{w'\rho'_i})_{\max}$. In our study we used the autocorrelation function to estimate the integral timescale.

Farmer et al. (2006) calculated fluxes of reactive nitrogen compounds and errors for their TD-LIF instrument by this method and could also specify the minimum detectable fluxes. Finkelstein and Sims (2001) showed that in general Eq. (8) is a reliable estimation for unstable and neutral conditions, although – for example – Eq. (8) tends to possibly underestimate the fractional flux sampling error by about 25% for the sensible heat flux. A possible overestimation up to about 30% is reported for the fluxes of H$_2$O and CO$_2$ (Finkelstein and Sims, 2001). Note that (σ_F/F_i) increases with increasing τ_F and decreases with increasing r_{wc}. On the basis of earlier measurements at this site, an estimation of this fractional flux sampling error is given and compared to results obtained during ECHO 2003 in Sect. 5.2. Note that all fluxes in this paper are given without correction for this systematic error.

4 Data analysis

The first to fourth moments (mean, variance, skewness, kurtosis) (Figs. 5 and 6) are calculated for the three wind vector components, the temperature as well as isoprene, MVK + MACR, monoterpenes, OH and HO$_2$ together with their mixed moments (second to fourth order) according to Beier and Weber (1992), Foken et al. (1995) and Cava et al. (2006). For the present discussion, second moments are of special interest, i.e. variances and covariances according to Eq. (7) like the local vertical flux densities $\overline{w'\rho'_i}$, the correlation $\overline{T'\rho'_i}$ between temperature T and ρ_i, and of trace gas compounds i, j in $(\overline{\rho_i'\rho'_j})$ according to Eq. (6). $\overline{T'\rho'_i}$ describes the local correlation between the temperature and partial densities of trace compounds, which may give hints towards the spatial distribution of their sinks and sources. The covariance $\overline{\rho_i'\rho'_j}$ (or its normalized value $I_s = \overline{\rho'_i\rho'_j}/\overline{\rho_i}\cdot\overline{\rho_j}$) indicates how well the gaseous compounds are mixed (e.g. Builtjes et al. 1987; Verver et al., 2000; Vinuesa et al., 2005; Ebel et al., 2007). Note that in all calculations of covariances, BVOCs are specified in units of mixing ratios (ppbv) and radicals in units of number densities (cm^{-3}).

5 Results

5.1 Mean values and higher moments

The time period between 09:00 to 15:00 CET on 25 July 2003 was characterized by cloudy conditions (Fig. 1) with a moderate horizontal wind velocity variation (Fig. 3) and slightly unstable to neutral stratification above the canopy. The broken clouds caused significant fluctuations of all radiation quantities above canopy, as is shown for the net radiation, Rn, and $J(O^1D)$ in Fig. 1. The air temperature T increased from 19 °C to 26.5 °C, while the specific humidity q increased only slightly from 09:00 to 12:00 CET up to about 9.5 g kg^{-1} and then decreased to about 8 g kg^{-1} (Fig. 2). The variability of solar radiation is reflected in the correlated low-frequency variations of OH on a time scale of 10 min to 30 min (Figs. 4 and 5), which can be explained by the primary, photochemical production of OH (Kleffmann et al., 2005). The measured HO$_2$ behaves differently compared to OH (Fig. 5) and increases stepwise following the temperature record (Fig. 2). Temperature ramp-like structures (Figs. 2 and 6b) occurred after 09:30 CET, when net radiation peaked (Fig. 1) and wind turned to a sector from W-SW to SE, in parallel to maxima in HO$_2$ (Fig. 5b) and isoprene (Fig. 6c). For this sector W-SW the footprint determined by Aubrun et al. (2005) showed that more than 90% of the emitted BVOCs originate from trees at distances up to 1500 m from the main tower. Comparable results are obtained for the wind sector SSW–SE.

The ramp like structures are mostly driven by variations in net radiation and are not driven entirely by wind shear at canopy top. The arithmetic mean values of the ratio (MVK + MACR)/isoprene =0.52 at 09:00–12:00 CET and 0.26 at 12:00–15:00 CET hint towards a changing influence of photochemical processes and advection, but are at the upper end of data obtained at daytime by Schaub (2007) and Spirig et al. (2005). Following the discussion by Schaub (2007) and Aubrun et al. (2005), this result suggests that for wind velocities below 3 m s^{-1} (Fig. 3) the residence times of BVOCs in CA are about 8 min to 20 min before the measuring point is reached.

Most data points of the OH and HO$_2$ concentrations are within the $\pm 2\sigma$ interval and are above the detection limits given in Sect. 3.3 (Fig. 4). The same holds for temperature, humidity and vertical velocity (Fig. 6a, b) as well as the organic compounds (Fig. 6c, d). Therefore, the number of data points outside this limits is smaller than 4%. For both radicals, the standard error Δa is below 10% of their arithmetic means and the relation $\sigma_x/\overline{x} < 0.42$ holds for each 10 min interval. The latter relation suggests also that Taylor's hypothesis is valid for these chemical species (Stull, 1988). Skewness (Sk) as well as kurtosis (Kur) point towards near normally distributed data with $Sk \approx 0$ and $Kur \approx 3$ (Fig. 5a, b). This is not the case for $J(O^1D)$ which shows a significant deviation from the characteristics of a normal distribution. The covariance between $J(O^1D)$ and OH is always positive with

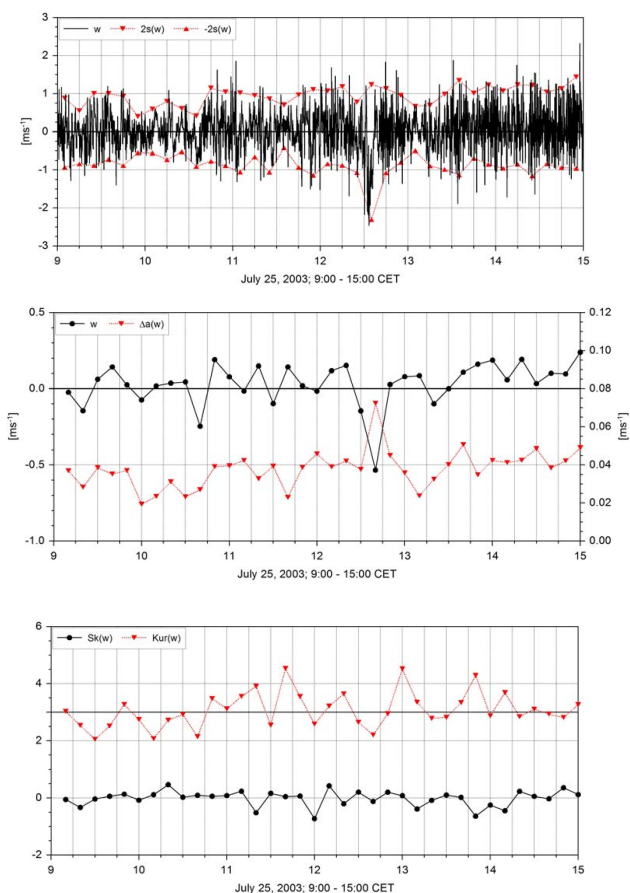**Fig. 6a.** Vertical velocity w (m s^{-1}) with the $\pm 2\sigma$-limits the mean value, the standard error Δa (right ordinate), the skewness Sk and the kurtosis Kur at 37 m height from a sonic anemometer for 25 July 2003, 09:00–15:00 CET.

Fig. 6b. Temperature T (K) with the $\pm 2\sigma$-limits the mean value, the standard error Δa (right ordinate), the skewness Sk and the kurtosis Kur at 37 m height from a sonic anemometer for 25 July 2003, 09:00–15:00 CET.

only small correlation coefficients, $r \leq 0.5$, and even two intervals with $r \approx 0$ on a time scale up to 10 min (Fig. 8). This is in contrast to the lower-frequency OH variations occuring on a time scale of 10 min to 30 min, which are well correlated with $J(\text{O}^1\text{D})$ (cf. Figs. 1 and 5a). The low correlation of OH and $J(\text{O}^1\text{D})$ for the shorter time periods is partly caused by instrumental noise and possibly by fast OH variations as a result of fluctuations of OH precursors and reactants.

Other quantities like vertical wind velocity w (Fig. 6a), temperature T (Fig. 6b) and organic compounds (Fig. 6c–e) mainly show a different statistical behaviour with respect to the higher moments Sk and Kur. Most of the w data are still near normally distributed, but occasionally show values with $Kur \geq 4$. Temperature data show $Sk > 0$ until about 13:40 CET, with a number of events with $Kur > 4$. This hints towards a more peaked distribution than a normal distribution in atmospheric turbulence (Sachs und Hedderich, 2006; Hollinger and Richardson, 2005), but with a large number of data points ($Sk > 0$) smaller than the arithmetic mean, especially for T until 13:40. The temperature data point towards
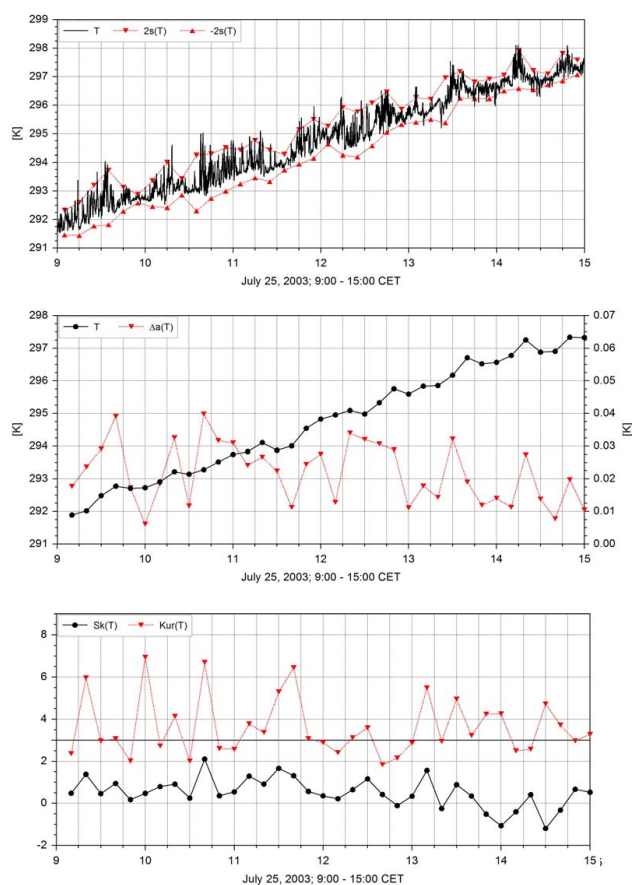
short events of heating the canopy by increased net radiation while the probability distribution function of the vertical velocity points towards conditions with only little development of convection which should show a positively skewed function. Comparable results with $Sk > 0$ are obtained for BVOCs with more data points smaller than the arithmetic means and even more peaked distributions ($Kur > 4$) during some periods. The third and fourth moments $Sk > 1$ and $Kur > 4$ for organic compounds are found only in time intervals with lower mixing ratios. Comparing the statistics for w and trace substances in most 10 min intervals, the small values below the mean occur simultaneously. Therefore, according to Eq. (7), the covariances between w and ρ_i (respectively the mixing ratio c_i) are also expected to be small for most 10 min intervals, which is confirmed in Figs. 7 and 9. Note that homogeneously mixed conditions are characterized by $Sk \approx 0$ and $Kur \approx 3$ (e.g. Warhaft, 2000). Therefore, one might expect some deviation of the segregation term in Eq. (6) from $I_s = 0$, at least for the system OH + isoprene (see Sect. 5.3).
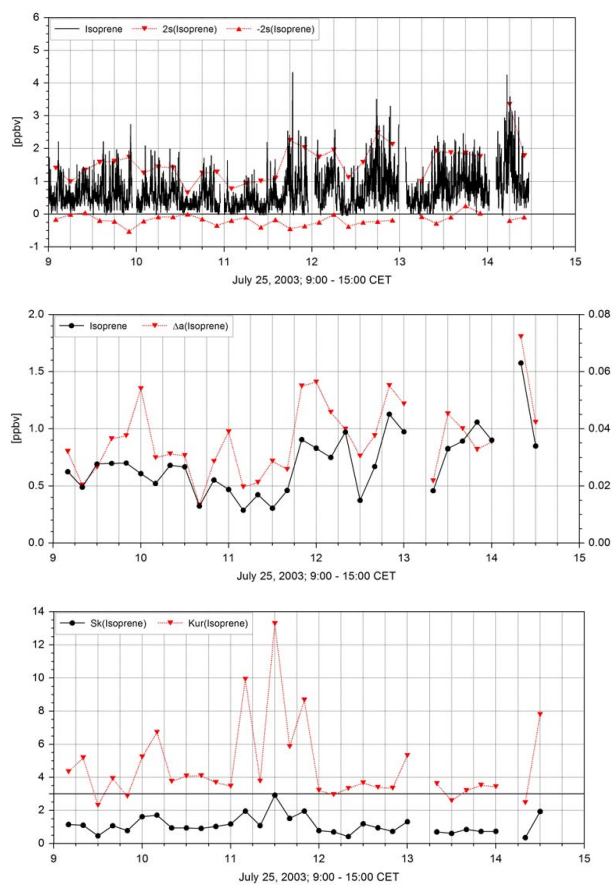
Fig. 6c. Mixing ratio of isoprene (ppbv) with the $\pm 2\sigma$-limits, the mean value, the standard error Δa (right ordinate), the skewness Sk and the kurtosis Kur, measured at 37 m height by PTR-MS on 25 July 2003, 09:00–15:00 CET.
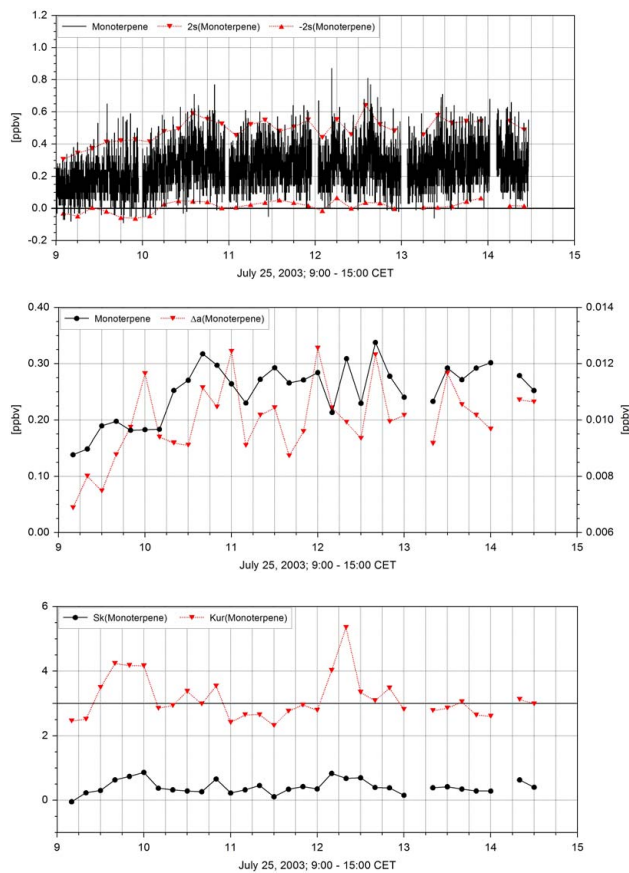
Fig. 6d. Mixing ratio of sum of monoterpenes (ppbv) with the $\pm 2\sigma$-limits, the mean value, the standard error Δa (right ordinate), the skewness Sk and the kurtosis Kur, measured at 37 m height by PTR-MS on 25 July 2003, 09:00–15:00 CET.

5.2 Covariances and fluxes

5.2.1 Experimental results

The fluxes of isoprene, the sum of monoterpenes, MVK + MACR, OH and HO₂ are given for 10 min averaging time in Fig. 7 together with the sensible heat flux. The precisions of the fluxes are 24–30% for OH and HO₂, and about 14% for BVOCs. During the slightly unstable to neutral stratified period of this day, characterized by negative values of L_*, the sensible heat flux is mainly directed upwards. Significant emission fluxes of BVOCs are found only around noon reaching maximum values of 0.2 ppbv ms⁻¹ (0.56 µg m⁻² s⁻¹) for isoprene, 0.04 ppbv ms⁻¹ (0.22 µg m⁻² s⁻¹) for monoterpenes, and 0.024 ppbv ms⁻¹ (0.07 µg m⁻² s⁻¹) for MVK + MACR. These values are about 20% larger than the corresponding noontime values for isoprene and monoterpenes reported by Spirig et al. (2005) for the same measurement site on 17 July 2003, a day with comparable meteorological con-

ditions. Unlike in the present work, Spirig et al. (2005) applied a spectral loss correction in the high-frequency range. If such a correction would be applied to our data, a systematic increase of the specific fluxes of 20%–42% would result at the main tower (Table 1). The error analysis in Sect. 3.5 describes the loss of higher frequencies in the flux calculation and its contribution to the total underestimation of fluxes F_i. Given $\tau_F \approx 2$ s, the error calculated by Eq. (8) yields a systematic mean underestimation of fluxes by 23% for isoprene, 33% for monoterpenes and 35% for MVK + MACR (Table 1). For OH and HO₂ the fluxes are underestimated by 37% and 31%, respectively for the period 09:00–15:00 CET, which is mainly caused by the correlation coefficients in the range of $0.2 < r_{wc} < 0.4$.

The fractional flux sampling errors can be compared with those calculated from data given by Spirig et al. (2005). For example, for $\tau_F = 2$ s and $r_{wc} = 0.2$ at mass 33 (ethanol) in their work, a value $(\sigma_F / F) \approx 41.6\%$ is obtained. For $\tau_F \approx 2.5$ s and $r_{wc} = 0.4$ at mass 69 (isoprene), the fractional flux sampling error is about $(\sigma_F / F_i) \approx 22\%$. Therefore, even with a
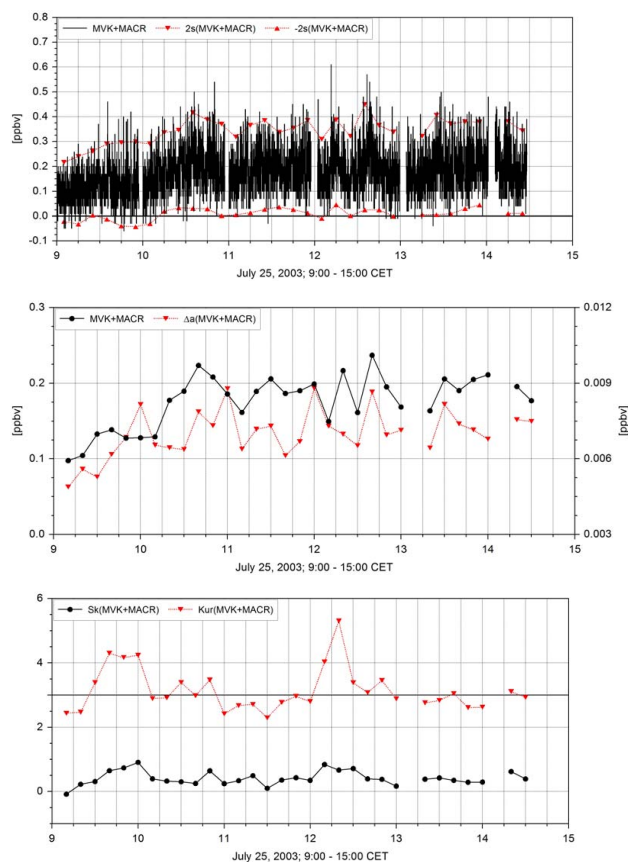
Fig. 6e. Mixing ratio of methyl vinyl ketone + methacrolein (MVK+MACR; in ppbv) with the $\pm 2\sigma$-limits, the mean value, the standard error Δa (right ordinate), the skewness Sk and the kurtosis Kur, measured at 37 m height by PTR-MS on 25 July 2003, 09:00–15:00 CET.

Fig. 7. Covariances (fluxes) of sensible heat, isoprene, sum of monoterpenes, MVK + MACR, OH and HO_2 at 37 m height for 25 July 2003, 09:00–15:00 CET.

Fig. 8. Covariances ($\overline{OH'_i \, J(O^1D)'_i}$) and correlation coefficient at 37 m height for 25 July 2003, 09:00–15:00 CET.

configuration of instruments, which only detect signals below about 0.25 Hz (Spirig et al., 2005), a reliable estimation of the flux can be performed. This result is also valid for our configuration during ECHO 2003, when we used the sonic anemometer together with the LIF and the PTR-MS (Sects. 2.3, 3.1–3.5) at a limiting frequency of 0.20 Hz. A corresponding analysis was also performed for the sensible heat flux H at $z/h_c \approx 1.23$ by comparing 10 Hz flux data and filtered 0.20 Hz data. At a measuring height of 37 m, the filtered data are only 14% lower than the 10 Hz data, which is comparable to the maximum loss of about 13% expected by Moore's spectral correction (Moore, 1986).

Beier and Weber (1992) or Finnigan et al. (2003) also discussed the contribution of low frequency fluctuations to the fluxes. The signals with the lower frequencies are sampled with less probability, and, therefore, have higher statistical uncertainty. The data presented cover averaging intervals of 10 min length within periods of 40–60 min. After each period, calibrations of the LIF and PTR-MS were performed (e.g. Figs. 4, 5a, 6c, d), also to prove a negligible change
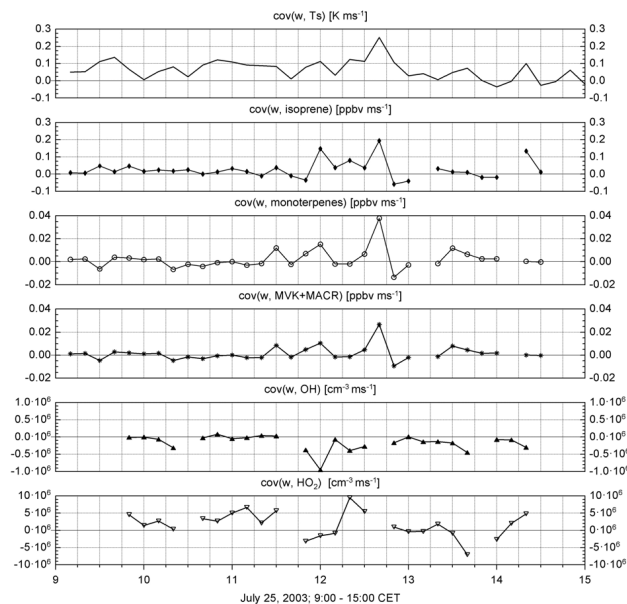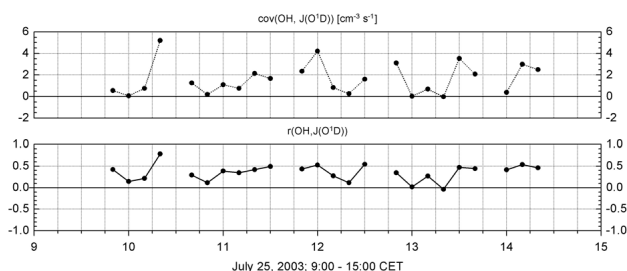
of the base line especially for LIF for conditions in the field (Fig. 4). The low frequency loss for the averaging intervals of 10 min was determined by the calculation of covariances for each of the longer periods (40–60 min) with lowest frequencies in the range $0.00028 \leq f \leq 0.00042$ Hz. Compared to the shorter averaging intervals of 10 min with $f = 0.0016$ Hz, the mean flux contribution for larger frequencies below that frequency is 22% $\pm 3\%$ (09:00–15:00 CET). The two studies (Beier and Weber, 1992; Finnigan et al., 2003) also show that the contribution to fluxes for $f < 0.0004$ Hz can be between 10%–20%. Therefore, the maximum low frequency loss for fluxes calculated for 10 min intervals may be up to 22%+10%$\approx$32%.

Although OH is considered to be a short-lived compound (Sect. 5.1), statistically significant fluxes have been detected above canopy top. The direction of the fluxes is downward and the maximum amount is 1×10^6 cm^{-3} ms^{-1}
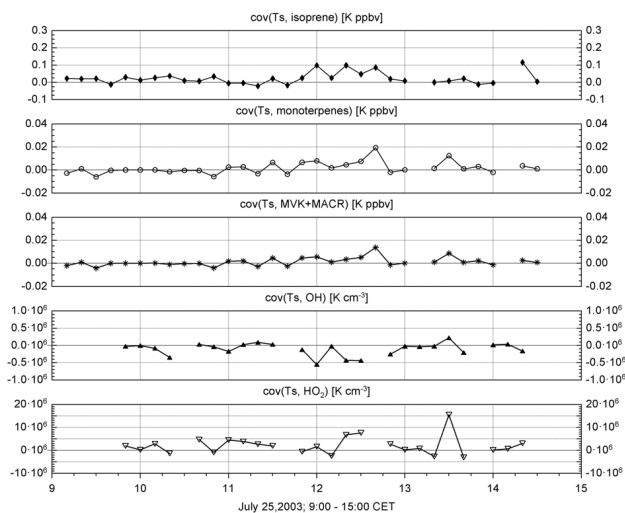
Fig. 9. Covariances $(\overline{T'_s c'_i})$ with $c'_i =$ isoprene, sum of monoterpenes, MVK + MACR, OH and HO$_2$ at 37 m height for 25 July 2003, 09:00–15:00 CET.

at 12:00 CET (Fig. 7). The flux direction is plausible since the canopy is a source of BVOCs including isoprene and monoterpenes, which react easily with OH. The calculated fluxes of HO$_2$ are larger than of OH. They were mostly directed upwards, reaching a maximum amount of 1×10^7 cm^{-3} ms^{-1}, but partly also downwards with a maximum amount of 7×10^6 cm^{-3} ms^{-1}. The predominant upward direction points to a significant source of HO$_2$ in the canopy, where HO$_2$ is likely produced by reaction of OH with freshly emitted BVOCs and advected NO. Albeit the concentrations of OH and HO$_2$ differ by a factor of about 30, their maximum fluxes only differ by a factor of 7–10.

Additional information can be obtained from the covariances of the trace substances and temperature (Fig. 9), which show that whenever heat is transported upwards (positive values of the sensible heat flux), the same behaviour is found for BVOCs and in most cases for HO$_2$. However, fluctuations of OH and temperature are always negatively correlated (Fig. 9) and positive (upward) sensible heat fluxes are found in parallel to negative (downward) OH fluxes (Fig. 7). The correlation with the sensible heat flux can be explained by the fact that the surfaces of leaves near canopy top are heated by solar radiation. This effect stimulates BVOC emissions from the leaves, and, simultaneously, causes upward transport of air which is in contact with the canopy.

The specific turbulent flow characteristics near the upper part of a forest occasionally allow for downward transport by gusts against a mean concentration or temperature gradient (e.g. Raupach et al., 1996; Cava et al., 2006; Zelger et al., 1997). This results in negative fluxes over the duration of ten minutes averaging time. A first application of the quadrant analysis for momentum, heat and mass transport as proposed by Katul et al. (1997) shows that the negative fluxes of HO$_2$

were found during periods when sweeps (downdrafts) dominated the turbulent transport.

The time scale for air renewal in the upper canopy between 21 m and 30 m can be evaluated by a method described by Paw U et al. (1992), yielding values of $150\,\mathrm{s} \leq \tau_T \leq 600\,\mathrm{s}$. For the transport from canopy top (z_f) to the measuring height (z_R), Zelger et al. (1997) estimated the transport time by combining canopy turbulence length scales L_w and variance σ_w as determined by Raupach (1988) with a detection scheme for free, forced and mixed convection as applied by Jacobs et al. (1994). The results agree numerically with the timescale for turbulent diffusion $\tau_{TD} = L_w / \sigma_w$. Applying this concept, the transport time from z_f to z_R is estimated to be in the range $8\,\mathrm{s} \leq \tau_{TD} \leq 28\,\mathrm{s}$.

5.2.2 Terms of the balance equation

The measured trace gas fluxes and concentrations in this work can be used to estimate to which extent HO$_x$ and BVOCs are directly influenced by chemistry and transport above the canopy. Assuming horizontal homogeneity, a complete evaluation of the balance equation Eq. (5) for species i would require knowledge of the corresponding fluxes at two heights (z_f and z_R), as well as the vertical distribution of the chemical sources (Q_i) and sinks (S_i) between z_f and z_R (Section 2.1 and Appendix A). In our field study, however, we have measured fluxes and concentrations at only one height (z_R). Therefore, besides horizontal homogeneity, additional assumptions must be made in order to compare the relative influences of chemical reactions and turbulent transport on the trace gas budgets. This will be done in the following for isoprene, OH and HO$_2$ as examples.

Isoprene is locally emitted from the canopy and has no chemical sources in the atmosphere above the canopy. The reaction with OH is the dominant chemical sink during daytime. Therefore, the isoprene flux at canopy top (z_f) should be compensated by the sum of its flux measured at height z_R and its chemical sink by reaction with OH. The mean chemical lifetime for isoprene, calculated from the measured OH concentrations and the reaction rate constant for OH+isoprene (1×10^{-10} cm^3 s^{-1}; Atkinson et al., 2006) is in the order of 25 min at noon. This lifetime is large compared to the vertical transport time (≤ 28 s) from canopy top to z_R or even the time for air renewal (≤ 10 min) in the crown region (Sect. 5.2.1). The chemical sink term, calculated from the measured concentrations of OH and isoprene, varies from 1.4×10^{-4} ppbv s^{-1} up to 7.7×10^{-4} ppbv s^{-1} (11:00–13:00 CET). This is equivalent to a mean isoprene flux of (1–5.4)$\times 10^{-3}$ ppbv ms^{-1} over the height interval $z_R - z_f = 7$ m. This is much less than the correspondingly measured fluxes of isoprene in the range of 0.02–0.2 ppbv m s^{-1} (Fig. 7), indicating that the measured flux at z_R is a good proxy of the flux at canopy top.

For OH the situation is different. It is not emitted, but produced in the gas phase by photochemical reactions.

Furthermore, it is consumed by fast reactions with a variety of trace gases such as isoprene and monoterpenes (Fig. 6c, d), CO, NO_2, formaldehyde and other species (Amman et al., 2004; Spirig et al., 2005, Kleffmann et al., 2005; Schaub, 2007). Turbulent transport of OH may play a role, when the chemical sources and sinks, and thus OH show vertical gradients. Using measured trace gas concentrations, the average chemical OH lifetime is estimated to about $\tau_{ch}=0.19\,s$ at noon (11:00–13:00 CET). Given a mean vertical velocity of smaller than $\pm0.5\,ms^{-1}$ (Fig. 6a), OH is transported by less than one meter within its lifetime. We assume that possible gradients of OH and other trace gases are small over this distance (1 m) at 7 m above canopy. We further assume that the vertical net flux of OH in a $1\,m^3$ box around the measuring height at z_R is not much larger than the amount of the measured OH flux ($\leq 1\times10^6\,cm^{-3}\,m\,s^{-1}$). For comparison, the chemical OH sink ($3.4\times10^7\,cm^{-3}\,s^{-1}$), calculated from the mean measured OH concentration ($6.5\times10^6\,cm^{-3}$) and the estimated OH lifetime (0.19 s), is equivalent to an OH flux of $3.4\times10^7\,cm^{-3}\,m\,s^{-1}$ over a vertical distance of 1 m. This is more than 30 times larger than the vertical OH flux. It means that (1) the flux of OH is locally balanced by chemical sources and sinks and (2) direct transport of OH plays no important role for the local chemical OH budget at height z_R.

Similar to OH, atmospheric HO_2 has no emission sources and is produced and destroyed by gas phase reactions. The dominant sink reaction is HO_2+NO, resulting in an HO_2 lifetime of $\tau_{ch}=20\,s$ for a mean mixing ratio of 0.22 ppbv NO at noon (Schaub, 2007). In this case, the lifetime is in the range of the turbulent transport time ($8\,s \leq \tau_{TD} \leq 28\,s$) for crossing the distance of 7 m between measurement height and top of the canopy (Sect. 5.2.2). The chemical sink term calculated from the mean measured HO_2 concentration and the HO_2 lifetime is $2.5\times10^7\,cm^{-3}\,s^{-1}$ at z_R. If we assume, for simplicity, that the loss rate is nearly constant between z_f and z_R, then the chemical sink in the 7 m layer above the canopy is equivalent to an HO_2 flux of $1.8\times10^8\,cm^{-3}\,m\,s^{-1}$. This may be compared to the measured local fluxes of HO_2 at z_R of about $(0.2-1.0)\times10^7\,cm^{-3}\,ms^{-1}$ (Fig. 5b), which are up to 5.6% of the chemical loss term. This comparison suggests that the local balance of HO_2 is significantly influenced by both chemistry and transport, consistent with the relation $\tau_{ch} \approx \tau_{TD}$. Vertical transport of the radicals is expected to become even more important in and below the canopy, where substantial gradients were observed in the vertical concentration profiles of OH and HO_2 that were measured on other days during the ECHO campaign (A. Hofzumahaus, personal communication, 2010).

Although no vertical flux profiles are available for OH and HO_2, the order of magnitude of the vertical flux divergence in Eq. (5) can be estimated. This is done by comparing effective transfer velocities v_{Tr} calculated at z_R with common values for deposition velocities $v_D \leq 0.01\,ms^{-1}$ of trace substances (e.g. Wesely and Hicks, 2000). A normalization of fluxes by mean mixing ratios yields effective transfer velocities at the height z_R. The resulting values vary in the range of -0.02 to $+0.3\,m\,s^{-1}$ for isoprene, -0.05 to $+0.12\,m\,s^{-1}$ for monoterpenes, -0.02 to $+0.1\,m\,s^{-1}$ for MVK+MACR, -0.14 to $0\,m\,s^{-1}$ for OH, and -0.02 to $+0.06\,ms^{-1}$ for HO_2, with a negative sign resulting from downward fluxes (Fig. 7). The difference $v_{Tr}-v_D$ times the mean concentration can be substituted as an estimate for the flux divergence in Eq. (5). The negative values of local transfer velocities are larger than experimentally determined deposition velocities of many trace gases (e.g. Lenschow and Hicks, 1989) due to the reactivity of the species represented by the integral term in Eq. (5).

5.3 Segregation

Inhomogeneously mixed concentration fields can be found near emission sources (e.g. Komori et al., 1991; Krol et al., 2000; Wahrhaft, 2000; Patton et al., 2001), or under the influence of nonlocal intermittent transport of fluid elements, for example in the ML above a forest and in the CA (e.g. Raupach et al., 1996; Wahrhaft, 2000, Patton et al., 2001), and also if convection (e.g. Cava et al., 2006; Verver et al., 2000) suppresses instantaneous mixing (Ebel et al., 2007; Vinuesa, 2005; Vila-Guerau de Arellano, 2005). The latter effect can be observed if air parcels are transported more rapidly than the chemical constituents have time to mix. Among the BVOCs measured at the ECHO field site, isoprene has the largest OH reactivity assuming a homogeneous, well mixed condition with $I_s \equiv 0$, because its reaction rate constant and its mean concentration are both larger than of the sum of monoterpenes. The analysis using the 0.2 Hz time series shows that the segregation term I_s for the reaction OH + isoprene reaches values (Fig. 10), which are above the significance level of $I_s=-0.03$ valid for isoprene and monoterpenes. Thus, at measuring height, isoprene and OH react slower with each other up to 15% than for homogeneously mixed conditions. The reaction rate for monoterpenes is less influenced under these conditions and is reduced at most by 5%. If a correction for high frequencies is applied to the times series as proposed by Spirig et al. (2005), this would not significantly change these results.

The maximum reduction by 15% of the reaction rate of isoprene + OH is of similar size as the experimental value of 13% reported by Butler et al. (2008) for the mixed layer over the tropical forest at Guyana. Butler et al. (2008) calculated their value from concentrations of isoprene and OH that were measured with time resolutions of 2 s and 5 s, respectively, on board an aircraft in October 2005. They discuss that the spatial segregation effect was probably larger and not fully resolved by their measurements because of the fast flight speed of the aircraft. When using a global chemistry climate model, they require an effective reduction of the isoprene + OH reaction rate by 50% to explain the observed isoprene concentrations by their global model. For comparison, Krol et al. (2000) estimated that the destruction of surface-emitted
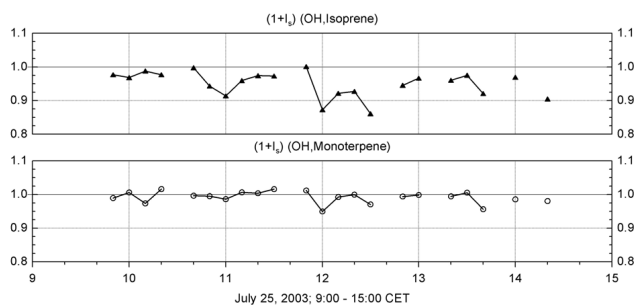
Fig. 10. Term $(1+I_s)$ according to Eq. 6 for OH and isoprene, and OH and the sum of monoterpenes.

hydrocarbons by OH may be slowed down by segregation up to 30% in the convective boundary layer. In the present work, the measured segregation effect is smaller despite the large heterogeneity expected in close proximity of the isoprene emitting canopy.

The magnitude of I_s presented in Fig. 10 is comparable to modelled results by Patton et al. (2001) for an isoprene emitting forest canopy with leaf area index comparable to the ECHO site. A time interval of 750 s is chosen in the model study for the calculation of higher moments. They also calculated a segregation intensity in the range of $0.01 \le I_s \le 0.16$ for a measuring height comparable to z_R with the smallest value for the Damköhler Number $Da = 0.02$ and the largest value for $Da = 0.17$. Compared to their definition of Da, the data from this study correspond to $0.01 \le Da \le 0.07$, and the segregation intensity for the reaction of OH with isoprene would be in the range $0.01 \le I_s \le 0.10$ compared to $0.01 \le I_s \le 0.15$ from the ECHO field study. Patton et al. (2001) also discuss that increasing scalar variance of the isoprene mixing ratio should cause an increase of I_s for the reaction with OH. Although a detailed comparison of their modelled and our experimental results has not been performed yet, it is already interesting to note that the largest values with $I_s \ge 0.08$ in Fig. 10 are found in intervals with highest scalar variance of isoprene mixing ratios. Note that a detailed analysis should also consider influences of the numerically modelled spatial heterogeneity of the BVOC emission (Krol et al., 2000) and the horizontal advection as in the wind tunnel study by Aubrun et al. (2005). In addition, the scalar velocity correlation coefficients (e.g. for fluxes of isoprene or heat) are larger by a factor of about two in the model study by Patton et al. (2001) compared to our data (Sect. 5.1) or other results from field experiments (e.g. Kaimal and Finnigan, 1994).

Further analysis shows that the covariance and the correlation coefficient between isoprene and monoterpenes are positive or zero. The correlation coefficient between OH and HO$_2$ is always near zero and shows only two exceptions. One negative value ($r=-0.29$) is encountered during the time period when the maximum OH concentration

is reached (12:15–12:30 CET) and $r(\mathrm{OH}, J(\mathrm{O}^1\mathrm{D}))$ is small, and one positive value ($r=0.32$) near 13:30 CET when both radicals have concentration maxima and $J(\mathrm{O}^1\mathrm{D})$ and $r(\mathrm{OH}, J(\mathrm{O}^1\mathrm{D}))$ are near maximum values.

6 Summary

The covariance method was applied for the first time to determine eddy fluxes of OH and HO$_2$, as well as segregation of OH and BVOCs (isoprene, monoterpenes) closely above a mixed deciduous forest. The covariance products were calculated for 10 min intervals from radical measurements performed by LIF, from BVOC measurements recorded by PTR-MS and horizontal and vertical wind from a sonic anemometer. All instruments were operated simultaneously at 7 m above the forest canopy, which had a top height of 30 m above ground, during the intensive field campaign ECHO 2003 in Jülich, Germany. Accuracy and precision of the covariances were mainly limited by the spatial separation of the measurements and the sampling frequency (0.2 Hz) of the LIF and PTR-MS instruments. The calculated fluxes of OH and HO$_2$ have precisions between 24%–30% and are systematically underestimated on average by about 37% and 31% at frequencies above 0.2 Hz, respectively. In addition, the low frequency part of the fluxes are also underestimated up to 32%. Though these errors are not small, the results of this first attempt to estimate covariance products of short-lived radicals are very promising.

OH was found to be transported mainly in the direction of chemical sinks, but its flux is small and locally compensated by chemical sink and source reactions. The fluxes of HO$_2$ are influenced by chemical reactions. They are often pointing to situations when HO$_2$ is transported upwards from the canopy to the overlaying atmosphere. The upward directed HO$_2$ transport is well correlated with the upward sensible heat flux, while the local OH flux is anticorrelated with the sensible heat flux. An analysis of the segregation term points to processes which cause inhomogeneous mixing of isoprene and OH near the canopy top, reducing the effective reaction rate up to 15%. Qualitatively this agrees with results from modelling by Patton et al. (2001). Segregation for OH and the sum of monoterpenes played an almost insignificant role ($<$5%) during this case study. Upward directed fluxes of isoprene and its photochemical oxidation products MVK and MACR were determined. The observations support the hypothesis that inside the canopy atmosphere, a significant amount of BVOCs can be chemically transformed and reaction products like HO$_2$ and MVK + MACR are emitted into the adjacent atmosphere. The present study suggests that the vertical flux and segregation effect had a notable, but relatively small effect on the local budget of OH at the chosen measurement position above canopy. Also this finding agrees with results from model studies for specific conditions of turbulent exchange and chemical reactivity. The situation may

be different at other locations below canopy top of the forest, which had an inhomogeneous distribution of different tree species with varying emission source strength of BVOCs, and where vertical gradients of HO_x were observed. Further studies using highly time resolved LIF measurements at different positions in a forest stand are required to improve the knowledge of the size and extent of these processes. If applied in further experiments, smaller distances between the sonic anemometer and the inlets of the instruments would ensure a significant reduction of the systematic underestimate of covariances. The baseline stability of LIF and PTR-MS is proven to be good enough for measurements up to about one hour. This allows now the calculation of higher order moments to cover also the low frequency part. In addition, the contribution of this spectral range to fluxes and segregation can be further studied based on experimental data. An analysis of the impact of the reported results on the local photochemistry and on modelled HO_x concentrations is subject of a forthcoming study.

Appendix A

Mathematical background

The basic concept how to perform measurements in the atmospheric flow above the Earth surface is derived from the local mass balance equation for the ith constituent (e.g. de Groot and Mazur, 1969; Businger, 1986; Kramm and Meixner, 2000; Kramm et al., 2008) per unit volume for a macroscopic flow. This reads

$$\frac{\partial \rho_i}{\partial t} + \nabla \cdot (\rho_i \boldsymbol{v} + \boldsymbol{J}_i) = Q_i - S_i. \tag{A1}$$

Here, the term $\partial \rho_i / \partial t$ is the local derivative of the partial density ρ_i with respect to time, $\boldsymbol{v}$ is the vector of the barycentric velocity (here the wind vector), $\boldsymbol{J}_i = \rho_i (\boldsymbol{v}_i - \boldsymbol{v})$ is the diffusion flux density (hereafter, a flux density is simply denoted as a flux), $\boldsymbol{v}_i$ is the individual velocity, and ∇ is the nabla or del operator expressed, for instance, in Cartesian coordinates by $\nabla = \boldsymbol{i} \frac{\partial}{\partial x} + \boldsymbol{j} \frac{\partial}{\partial y} + \boldsymbol{k} \frac{\partial}{\partial z}$, where $\boldsymbol{i}$, $\boldsymbol{j}$ and $\boldsymbol{k}$ are the unit vectors in west-east ($\boldsymbol{x}$), south-north ($\boldsymbol{y}$), and vertical ($\boldsymbol{z}$) direction, respectively. Furthermore, Q_i represents the sources and S_i the sinks of matter in the fluid due to chemical reactions and/or phase transition processes. Note, an emission or deposition enters into Eq. (A1) by boundary condition. Moreover, the quantities $\rho_i \boldsymbol{v}$ and $\boldsymbol{J}_i$ are frequently called the convective and nonconvective transports of matter, respectively. Summing Eq. (A1) over all substances from $i = 0, \ldots, k$ leads to the macroscopic balance equation for the total mass per unit volume customarily called the equation of continuity (e.g. Landau and Lifshitz, 1959),

$$\frac{\partial \rho}{\partial t} + \nabla \cdot (\rho \boldsymbol{v}) = 0, \tag{A2}$$

where the density of air is given by

$$\rho = \sum_{i=0}^{k} \rho_i \tag{A3}$$

and the vector of the barycentric velocity by

$$\boldsymbol{v} = \frac{1}{\rho} \sum_{i=0}^{k} \rho_i \boldsymbol{v}_i. \tag{A4}$$

The local mass balance equation for a turbulent flow Eq. (2) can be derived by using Reynolds' averaging calculus, i.e. decomposition of any instantaneous field quantity $\varphi(\boldsymbol{r})$ like $\rho_i(\boldsymbol{r})$, $\rho(\boldsymbol{r})$, and $\boldsymbol{v}(\boldsymbol{r})$ by $\varphi(\boldsymbol{r}) = \overline{\varphi} + \varphi'$ and subsequent averaging according to (e.g. van Mieghem, 1949, 1973; Herbert, 1975; Kramm and Meixner, 2000; Kramm et al., 2008).

$$\overline{\varphi} = \overline{\varphi}(\boldsymbol{r}) = \frac{1}{G} \int_{G} \varphi(\boldsymbol{r}, \boldsymbol{r}') dG', \tag{A5}$$

where $\overline{\varphi}$ is the ensemble average of $\varphi(\boldsymbol{r})$, and the fluctuation φ' is the difference between the former and the latter. Here, $\boldsymbol{r}$ is the four-dimensional vector of space and time in the original coordinate system, $\boldsymbol{r}'$ is that of the averaging domain G where its origin, $\boldsymbol{r}' = 0$, is assumed to be $\boldsymbol{r}$, and $dG' = d^3\boldsymbol{r}' dt'$. The averaging domain G is given by $G = \int_G dG'$. Hence, the quantity $\overline{\varphi}$ represents the mean values of $\varphi(\boldsymbol{r})$ for the averaging domain G at the location $\boldsymbol{r}$. Since $\overline{\overline{\varphi}} = \overline{\varphi}$ (e.g. van Mieghem, 1949, 1973; Herbert, 1975; Kramm et al., 1995), averaging the quantity $\varphi(\boldsymbol{r}) = \overline{\varphi} + \varphi'$ provides $\overline{\varphi'} = 0$.

In accord with the ergodic theorem, ensemble average as expressed by Eq. (A5) may be replaced in practice by time average (Liepmann, 1952). But a basic requirement for using a time averaging procedure is that turbulence is statistically steady (e.g. Falkovich and Sreenivasan, 2006; Lumley and Panofsky, 1964; Tennekes and Lumley, 1972). Consequently, sophisticated procedures for identifying and eliminating non-stationary effects (trends) are indispensable to prevent that computed eddy fluxes of atmospheric constituents are notably affected by non-stationary effects. For our further considerations we suppose that steady-state conditions prevail, i.e. that any local derivative with respect to time is considered as negligible. But this requires the application of the detrending method in the data analysis (see Sects. 3.5 and 4) to eliminate non-stationary contributions to flux densities F_i and other moments.

Applying Reynolds' averaging calculus to Eq. (A1) yields Eq. (A6) respectively Eq. (2) (e.g. Businger, 1986; Kramm and Meixner, 2000; Kramm et al., 2008)

$$\frac{\partial \overline{\rho_i}}{\partial t} + \nabla \cdot \left(\overline{\rho_i} \ \overline{\boldsymbol{v}} + \overline{\rho_i' \boldsymbol{v}'} + \overline{\boldsymbol{J}_i} \right) = \overline{Q_i} - \overline{S_i}. \tag{A6}$$

For the equation of continuity we obtain

$$\frac{\partial \overline{\rho}}{\partial t} + \nabla \cdot \left(\overline{\rho} \ \overline{\boldsymbol{v}} + \overline{\rho' \boldsymbol{v}'} \right) = 0. \tag{A7}$$

Within the framework of the Boussinesq approximation the term including turbulent fluctuations of ρ, $\overline{\rho'\boldsymbol{v}'}$, is considered as negligible in comparison with the term $\overline{\rho}\ \overline{\boldsymbol{v}}$ so that we have

$$\frac{\partial \overline{\rho}}{\partial t} + \nabla \cdot (\overline{\rho}\ \overline{\boldsymbol{v}}) \cong 0. \tag{A8}$$

If we assume that Eq. (A2) or Eq. (A8) can be approximated by $\nabla \cdot \boldsymbol{v} = 0$ (the condition of an incompressible fluid), we will have $\nabla \cdot \overline{\boldsymbol{v}} = 0$ and $\nabla \cdot \boldsymbol{v}' = 0$ (e.g. Landau and Lifshitz, 1959; Monin and Yaglom, 1971; Kramm and Mölders, 2005). As discussed in the text, if we further assume that the fields of the wind velocity and the partial densities of the atmospheric constituents are horizontally homogeneously distributed we will obtain Eqs. (2) and (4). As mentioned, from Eq. (4) we may infer that $\overline{w}$ is constant with height. Since at any rigid surface $\overline{w}$ is equal to zero, we may state that $\overline{w}$ is generally equal to zero under the conditions that the fluid is incompressible and horizontally homogeneous. In a fully turbulent flow (but not at the boundaries) the diffusion flux of a gaseous entity can be neglected because $\left|\overline{\rho_i'w'}\right| \gg \left|\overline{J_{i,z}}\right|$ and under these premises Eq. (3) amounts to Eq. (5) or Eq. (A9)

$$\left(\overline{\rho_i'w'} + \overline{J_{i,z}}\right)_{z=z_f} = \overline{\rho_i'w'}\Big|_{z=z_R} - \int_{z_f}^{z_R} \left(\overline{Q_i} - \overline{S_i}\right)dz. \tag{A9}$$

For this concept, the emission or deposition of trace substances is given by the boundary conditions at heights $z=z_f$. Only in the case of long-lived gaseous species the second term of the right-hand side of Eq. (A9) can be neglected. Under these premises we obtain the so-called constant flux condition:

$$\left(\overline{\rho_i'w'} + \overline{J_{i,z}}\right)_{z=z_f} = \overline{\rho_i'w'}\Big|_{z=z_R}. \tag{A10}$$

Edited by: T. Karl

References

Amman, C., Spirig, C., Neftel, A., Steinbacher, M., Komenda, M., and Schaub, A.: Application of PTR-MS for measurements of biogenic VOC in a deciduous forest, Int. J. Mass Spectrom., 239, 87–101, 2004.

Astarita, G.: Mass transfer with chemical reaction, Elsevier, Amsterdam, 1967.

Atkinson, R. and Arey, J.: Gas-phase tropospheric chemistry of biogenic volatile organic compounds: a review, Atmos. Environ., 37, S197–S229, 2003.

Atkinson, R., Baulch, D. L., Cox, R. A., Crowley, J. N., Hampson, R. F., Hynes, R. G., Jenkin, M. E., Rossi, M. J., Troe, J., and IUPAC Subcommittee: Evaluated kinetic and photochemical data for atmospheric chemistry: Volume II – gas phase reactions of organic species, Atmos. Chem. Phys., 6, 3625–4055, doi:10.5194/acp-6-3625-2006, 2006.

Aubrun, S., Koppmann, R., Leitl, B., Möllmann-Coers, M., and Schaub, A.: Physical modelling of a complex forest area in a wind tunnel – comparison with field data, Agr. Forest. Meteorol., 129, 121–135, 2005.

Beier, N. and Weber, M.: Turbulente Austauschprozesse in der Grenzschicht. Meteorologisches Institut, Universität München, Germany, 181 pp., 1992.

Bohn, B., Kraus, A., Müller, M., and Hofzumahaus, A.: Measurement of atmospheric O$_3\rightarrow$O^{1}D photolysis frequencies using filterradiometry, J. Geophys. Res., 109, D10S90, doi:10.1029/2003JD004319, 2004.

Bohn, B.: Solar spectral actinic flux and photolysis frequency measurements in a deciduous forest, J. Geophys. Res., 111, D15303, doi:10.1029/2005JD006902, 2006a.

Bohn, B., Koppmann, R., and Rohrer, F.: Seasonal variations and profile measurements of photolysis frequencies j(O^{1}D) and j(NO$_2$) at the ECHO forest field site, J. Geophys. Res., 111, D12303, doi:10.1029/2005JD006856, 2006b.

Bouvier-Brown, N. C., Goldstein, A. H., Gilman, J. B., Kuster, W. C., and de Gouw, J. A.: In-situ ambient quantification of monoterpenes, sesquiterpenes, and related oxygenated compounds during BEARPEX 2007: implications for gas- and particle-phase chemistry, Atmos. Chem. Phys., 9, 5505–5518, doi:10.5194/acp-9-5505-2009, 2009.

Builtjes, P. J. H. and Talmon, A. M.: Macro- and microscale mixing in chemical reactive plumes, Bound.-Lay. Meteorol., 41, 417–426, 1987.

Businger, J. A.: Evaluation of the accuracy with which dry deposition can be measured with current micrometeorological techniques, J. Clim. Appl. Meteorol., 25, 1100–1124, 1986.

Butler, T. M., Taraborrelli, D., Brühl, C., Fischer, H., Harder, H., Martinez, M., Williams, J., Lawrence, M. G., and Lelieveld, J.: Improved simulation of isoprene oxidation chemistry with the ECHAM5/MESSy chemistry-climate model: lessons from the GABRIEL airborne field campaign, Atmos. Chem. Phys., 8, 4529–4546, doi:10.5194/acp-8-4529-2008, 2008.

Carslaw, N., Creasey, D. J., Harrison, D., Heard, D. E., Hunter, M. C., Jacobs, P. J., Jenkin, M. E., Lee, J. D., Lewis, A. C., Pilling, M. J., Saunders, S. M., and Seakins, P. W.: OH and HO$_2$ radical chemistry in a forest region of north-western Greece, Atmos. Environ., 35, 4725–4737, 2001.

Cava, D., Katul, G. G., Scrimieri, A., Poggi, D., Cescatti, A., and Giostra, U.: Buoyancy and the sensible heat flux budget within

dense canopies, Bound.-Lay. Meteorol., 118, 217–240, 2006.

Damköhler, G.: Einfluß von Diffussion, Strömung und Wärmetransport auf die Ausbeute bei chemisch-technischen Reaktionen, VDI, Leverkusen, Germany, 126 pp., 1957.

de Groot, S. R. and Mazur, P.: Non-Equilibrium Thermodynamics, North-Holland Publishing Comp., Amsterdam/London, 541 pp., 1969.

Di Carlo, P., Brune, W. H., Martinez, M., Harder, H., Lesher, R., Ren, X., Thornberry, T., Carroll, M., Young, V., Shepson, P. B., Riemer, D., Apel, E., and Campbell, C.: Missing OH reactivity in a forest: evidence for unknown reactive biogenic VOCs, Science, 304, 722–725, 2004.

Dlugi, R.: Interaction of NO$_x$ and VOCs within vegetation, in: Proc. EUROTRAC-Symposium 1992, SPB Acad. Publ., The Hague, The Netherlands, 682–688, 1993.

Ebel, A., Memmesheimer, M., and Jakobs, H. J.: Chemical perturbations in the planetary boundary layer and their relevance for chemistry transport modelling, Bound.-Lay. Meteorol., 125, 256–278, 2007.

Ehhalt, D. H.: Photooxidation of trace gases in the troposphere, Phys. Chem. Chem. Phys., 1, 5401–5408, 1999.

Falkovich, G. and Sreenivasan, K. R.: Lessons from hydrodynamic turbulence, Phys. Today, 59(4), 43–49, 2006.

Farmer, D. K., Wooldridge, P. J., and Cohen, R. C.: Application of thermal-dissociation laser induced fluorescence (TD-LIF) to measurement of HNO$_3$, $\sum$alkyl nitrates, $\sum$peroxy nitrates, and NO$_2$ fluxes using eddy covariance, Atmos. Chem. Phys., 6, 3471–3486, doi:10.5194/acp-6-3471-2006, 2006.

Finkelstein, P. L. and Sims, P. F.: Sampling error in eddy correlation flux measurements, J. Geophys. Res., 106(D4), 3503–3509, 2001.

Finlayson-Pitts, B. J. and Pitts Jr., J. N.: Atmospheric Chemistry: Fundamentals and Experimental Techniques, J. Wiley & Sons, New York, Germany, 1098 pp., 1986.

Finnigan, J. J., Clement, R., Malhi, Y., Leuning, R., and Cleugh, H. A.: A re-evaluation of long-term flux measurement techniques. Part I: Averaging and coordinate rotation, Bound.-Lay. Meteorol., 107, 1–48, 2003.

Fitzjarrald, D. R. and Lenschow, D. H.: Mean concentration and flux profiles for chemically reactive species in the atmospheric surface layer, Atmos. Environ., 17, 2505–2512, 1983.

Foken, T., Dlugi, R., and Kramm, G.: On the determination of dry deposition and emission of gaseous compounds at the biosphere-atmosphere interface, Meteorol. Z., 4(NF), 91–118, 1995.

Forkel, R., Klemm, O., Graus, M., Rappenglück, B., Stockwell, W. R., Grabmer, W., Held, A., Hansel, A., and Steinbrecher, R.: Trace gas exchange and gas phase chemistry in a Norway spruce forest: A study with a coupled 1-dimensional canopy atmospheric chemistry emission model, Atmos. Environ., 40(S1), 28–42, 2006.

Fuentes, J. D., Lerdau, M., Atkinson, R., Baldocchi, D., Bottenheim, J. W., Ciccioli, P., Lamb, B., Geron, C., Gu, L., Guenther, A., Sharkey, T. D., and Stockwell, W.: Biogenic Hydrocarbons in the Atmospheric Boundary Layer: A Review, B. Am. Meteorol. Soc., 81, 1537–1575, 2000.

Gao, W., Wesely, M. L., and Doskey, P. V.: Numerical modeling of the turbulent-diffusion and chemistry NO$_x$, O$_3$, isoprene, and other reactive trace gases in and above a forest canopy, J. Geophys. Res., 98(D10), 18339–18353, 1993.

Guenther, A., Hewitt, C. N., Erickson, D., Fall, R., Geron, C., Graedel, T., Harley, P., Klinger, L., Lerdau, M., McKay, W. A., Pierce, T., Scholes, B., Steinbrecher, R., Tallamraju, R., Taylor, J., and Zimmerman, P.: A global model of natural volatile organic compound emissions, J. Geophys. Res., 100, 8873–8892, 1995.

Guenther, A., Karl, T., Harley, P., Wiedinmyer, C., Palmer, P. I., and Geron, C.: Estimates of global terrestrial isoprene emissions using MEGAN (Model of Emissions of Gases and Aerosols from Nature), Atmos. Chem. Phys., 6, 3181–3210, doi:10.5194/acp-6-3181-2006, 2006.

Hallquist, M., Wenger, J. C., Baltensperger, U., Rudich, Y., Simpson, D., Claeys, M., Dommen, J., Donahue, N. M., George, C., Goldstein, A. H., Hamilton, J. F., Herrmann, H., Hoffmann, T., Iinuma, Y., Jang, M., Jenkin, M. E., Jimenez, J. L., Kiendler-Scharr, A., Maenhaut, W., McFiggans, G., Mentel, Th. F., Monod, A., Prévôt, A. S. H., Seinfeld, J. H., Surratt, J. D., Szmigielski, R., and Wildt, J.: The formation, properties and impact of secondary organic aerosol: current and emerging issues, Atmos. Chem. Phys., 9, 5155–5235, doi:10.5194/acp-9-5155-2009, 2009.

Herbert, F.: Irreversible Prozesse der Atmosphäre – 3. Teil (Phänomenologische Theorie mikroturbulenter Systeme), Beitr. Phys. Atmos., 48, 1–29, 1975.

Hofzumahaus, A., Aschmutat, U., Hessling, M., Holland, F., and Ehhalt, D. H.: The measurement of tropospheric OH radicals by laser-induced fluorescence spectroscopy during the POPCORN field campaign, Geophys. Res. Lett., 23, 2541–2544, 1996.

Hofzumahaus, A., Rohrer, F., Keding, L., Birger, B., Brauers, T., Chang, C.-C., Fuchs, H., Holland, F., Kita, K., Kondo, Y., Li, X., Lou, S., Shao, M., Zeng, L., Wahner, A., and Zhang, Y.: Amplified trace gas removal in the troposphere, Science, 324, 1702–1704, 2009.

Holland, F., Hessling, M., and Hofzumahaus, A.: Insitu measurement of tropospheric OH radicals by laser-induced fluorescence – a description of the KFA instrument, J. Atmos. Sci., 52(19), 3393–3401, 1995.

Holland, F., Hofzumahaus, A., Schäfer, J., Kraus, A., and Pätz, H.-W.: Measurements of OH and HO$_2$ radical concentrations and photolysis frequencies during BERLIOZ, J. Geophys. Res., 108(D4a), 8246, doi:10.1029/2001JD001393, 2003.

Hollinger, D. Y. and Richardson, A. D.: Uncertainty in eddy covariance measurements and its application to physiological models, Tree Physiol., 25, 873–885, 2005.

Holzinger, R., Lee, A., Paw U, K. T., and Goldstein, U. A. H.: Observations of oxidation products above a forest imply biogenic emissions of very reactive compounds, Atmos. Chem. Phys., 5, 67–75, doi:10.5194/acp-5-67-2005, 2005.

Horst, T. W.: A simple formula for attenuation of eddy fluxes with first-order-response scalar sensors, Bound.-Lay. Meteorol., 82, 219–233, 1997.

Jacobs, A. F. G., Van Boxel, J. H., and El-Kilani, R. M. M.: Nighttime free convection characteristics within a plant canopy. Boundary Layer Meteorology, 71, 375–391, 1994.

Kaimal, J. C. and Finnigan, J. J.: Atmospheric Boundary layer Flows: Their Structure and Measurement, Oxford University Press, New York/Oxford, 289 pp., 1994.

Karl, T., Guenther, A., Spirig, C., Hansel, A., and Fall, R.: Seasonal variation of biogenic VOC emissions above a mixed hardwood

forest in northern Michigan, Geophys. Res. Lett., 30(23), 2186, doi:10.1029/2003GL018432, 2003.

Karl, T., Potosnak, M., Guenther, A., Clark, D., Walker, J., Herrick, J. D., and Geron, C.: Exchange processes of volatile organic compounds above a tropical rain forest: Implications for modeling tropospheric chemistry above dense vegetation, J. Geophys. Res., 109, D18306, doi:10.1029/2004JD004738, 2004.

Karl, T., Guenther, A., Yokelson, R. J., Greenberg, J., Potosnak, M., Blake, D. R., and Artaxo, P.: The tropical forest and fire emissions experiment: Emission, chemistry, and transport of biogenic volatile organic compounds in the lower atmosphere over Amazonia, J. Geophys. Res., 112, D18302, doi:10.1029/2007JD008539, 2007

Katul, G., Msieh, C.-I., Kuhn, G., Ellsworth, D., and Nie, D.: Turbulent eddy motion at the forest-atmosphere interface, J. Geophys. Res., 102(D12), 13407–13421, 1997.

Kesselmeier, J. and Staudt, M.: Biogenic volatile organic compounds (VOC): An overview on emission, physiology and ecology, J. Atmos. Chem., 33, 23–88, 1999.

Kleffmann, J., Gavriloaiei, T., Hofzumahaus, A., Holland, F., Koppmann, R., Rupp, L., Schlosser, E., Siese, M., and Wahner, A.: Daytime formation of nitrous acid: A major source of OH radicals in a forest, Geophys. Res. Lett., 32, L05818, doi:10.1029/2005GL022524, 2005.

Komori, S., Kanzaki, T., and Morakami, Y.: Simultaneous measurements on instantaneous concentrations of two reacting species in a turbulent flow with a rapid reaction, Phys. Fluids, A3, 507–510, 1991.

Kramm, G. and Dlugi, R.: Modelling of the vertical fluxes of nitric acid, ammonia, and ammonium nitrate in the atmospheric surface layer, J. Atmos. Chem., 18, 319–357, 1994.

Kramm, G., Dlugi, R., Dollard, G. J., Foken, T., Mölders, N., Müller, H., Seiler, W., and Sievering, H.: On the dry deposition of ozone and reactive nitrogen species, Atmos. Environ., 29, 3209–3231, 1995.

Kramm, G. and Meixner, F. X.: On the dispersion of trace species in the atmospheric boundary layer: A re-formulation of the governing equations for the turbulent flow of the compressible atmosphere, Tellus, 52A, 500–522, 2000.

Kramm, G. and Mölders, N.: On the transfer of momentum, sensible heat and matter across the interfacial sublayer over aerodynamically smooth surfaces, J. Calcutta Math. Soc., 1(3–4), 105–120, 2005.

Kramm, G., Dlugi, R., and Zelger, M.: On the recognition of fundamental physical principles in recent atmospheric-environmental studies, J. Calcutta Math. Soc., 4(1–2), 31–55, 2008.

Krol, M. C., Molemaker, M.-J., and Guerau de Arellano, J. V.: Effects of turbulence and heterogeneous emission on photochemically active species in the convective boundary layer, J. Geophys. Res., 105(D5), 6871–6884, 2000.

Kroll, J. H., Clarke, J. S., Donahue, N. M., Anderson J. G., and Demerjian, K. L.: Mechanism of HO$_x$ formation in the gas-phase ozone-alkene reaction, 1, Direct pressure-dependent measurements of prompt OH yields, J. Phys. Chem. A., 105, 1554–1560, 2001.

Landau, L. D. and Lifshitz, E. M.: Course of Theoretical Physics, Vol. 6, Fluid Mechanics, Pergamon Press, Oxford/New York/Toronto/Sydney/Paris/Frankfurt, 536 pp., 1959.

Lenschow, D. H. and Hicks, B. B.: Global Tropospheric Chemisty –

Chemical Fluxes in the Global Atmosphere, National Center for Atmospheric Research, Boulder, Colorado, USA, 107 pp., 1989.

Lenschow, D. H., Mann, J., and Kristensen, L.: How long is long enough when measuring fluxes and other turbulent statistics?, J. Atmos. Ocean. Tech., 11, 661–673, 1994.

Lenschow, D. H.: Micrometerological techniques for measuring biosphere-atmosphere trace gas exchange, in: Methods in Ecology; Biogenic Trace Gases: Measuring Emissions from Soil and Water, edited by: Matson, P. A. and Harris, R. C., 126–163, 1995.

Lippmann, H. V.: Aspects of the turbulence problem, Z. Angew. Math. Phys., 3, 1th part, 321–342, 2nd part, 407–426, 1952.

Lumley, J. L. and Panofsky, H. A.: Atmospheric Turbulence, Interscience Publishers, New York/London/Sydney, 239 pp., 1964.

Makar, P. A., Fuentes, J. D., Wang, D., Staebler, R. M., and Wiebe, M. A.: Chemical processing of biogenic hydrocarbons within and above a temperate deciduous forest, J. Geophys. Res., 104(D3), 3581–3603, 1999.

Monin, A. S. and Yaglom, A. M.: Statistical Fluid Mechanics, MIT Press, Cambridge, Mass., Vol. 1, 769 pp., 1971.

Moore, C. J.: Frequency response corrections for eddy correlation systems, Bound.-Lay. Meteorol., 37, 17–36, 1986.

Oncley, S. P.: Flux Parameterization Techniques in the Atmospheric Surface Layer, Dissertation, University of California, Irvine, CA, USA, 202 pp., 1989.

Patton, E. G., Davis, K. J., Barth, M. C., and Sullivan, P. P.: Decaying scalars emitted by a forest canopy: A numerical study, Bound.-Lay. Meteorol., 100, 91–129, 2003.

Paw U, K. T., Brunet, Y., Colineau, S., Shaw, R. H., Maitani, T., Qiu, J., and Hipps, L.: On turbulent coherent structures in and above agricultural plant canopies, Agr. For. Meteorol., 61, 55–68, 1992.

Poisson, N., Kanakidou, M., and Crutzen, P. J.: Impact of non-methane hydrocarbons on tropospheric chemistry and the oxidizing power of the global troposphere: 3-dimensional modelling results, J. Atmos. Chem., 36, 157–230, 2000.

Press, W. H., Flannery, B. P., Teukolsky, S .A., and Vetterling, W. T.: Numerical Recipes, Cambridge University Press, Cambridge, UK, 1991.

Raupach, M. R.: Canopy transport processes, in: Flow and Transport in the Natural Environment: Advances and Applications, edited by: Steffen, W. L. and Denmead, O. T., Springer, Berlin, Germany, 95–127, 1988.

Raupach, M. R., Finnigan, J. J., and Brunet, Y.: Coherent eddies and turbulence in vegetation canopies: The mixing layer analogy, Bound.-Lay. Meteorol., 78, 351–382, 1996.

Sachs, L. and Hedderich, J.: Angewandte Statistik, Springer, Berlin, Heidelberg, New York, 702 pp., 2006.

Sanderson, M. G., Jones, C. D., Collins, W. J., Johnson, C. E., and Derwent, R. G.: Effect of climate change on isoprene emissions and surface ozone levels, Geophys. Res. Lett., 30(18), 1936, doi:10.1029/2003GL017642, 2003.

Schaub, A.: Untersuchung von Isopren und dessen Oxidationsprodukten in und oberhalb eines Mischwaldes, Dissertation, Mathematisch-Naturwissenschaftliche Fakultät, Universität Köln, Germany, 2007.

Schotanus, P., Nieuwstadt, F. T. M., and de Bruin, H. A. R.: Temperature measurements with a sonic anemometer and its application to heat and moisture flux, Bound.-Lay. Meteorol., 26, 81–93, 1983.

Seinfeld, J. H. and Pandis, S. N.: Atmospheric Chemistry and Physics, John Wiley & Sons, New York/Chichester/Weilheim/Brisbane/Singapore/Toronto, 1326 pp., 1998.

Spirig, C., Neftel, A., Ammann, C., Dommen, J., Grabmer, W., Thielmann, A., Schaub, A., Beauchamp, J., Wisthaler, A., and Hansel, A.: Eddy covariance flux measurements of biogenic VOCs during ECHO 2003 using proton transfer reaction mass spectrometry, Atmos. Chem. Phys., 5, 465–481, doi:10.5194/acp-5-465-2005, 2005.

Stockwell, W. R.: Effects of turbulence on gas-phase atmospheric chemistry: Calculation of the relationship between time scale for diffusion and chemical reaction, Meteorol. Atmos. Phys., 57, 159–171, 1995.

Stroud, C., Makar, P., Karl, T., Guenther, A., Geron, C., Turnipseed, A., Nemitz, E., Baker, B., Potosnak, M., and Fuentes, J. D.: Role of canopy-scale photochemistry in modifying biogenic-atmosphere exchange of reactive terpene species: Results from the CELTIC field study, J. Geophys. Res., 110, D17303, doi:10.1029/2005JD005775, 2005.

Stull, R. B.: Introduction to Boundary Layer Meteorology, Kluwer Academic Publisher, Dordrecht/Boston/London, 666 pp., 1988.

Sun, J.: Tilt correction over complex terrain and their implication for CO$_2$-transport, Bound.-Lay. Meteorol., 124, 143–159, 2007.

Tan, D., Faloona, I., Simpas, J. B., Brune, W., Shepson, P. B., Couch, T. L., Sumner, M. A., Thornberry, T., Apel, E., Riemer, D., and Stockwell, W.: HO$_x$-budgets in a deciduous forest: Results from the PROPHET summer 1998 campaign, J. Geophys. Res., 106, 24407–24427, 2001.

Tennekes, H. and Lumley, J. L.: A First Course in Turbulence, MIT Press, Cambridge, MA, USA, 300 pp., 1972.

Toor, H. L.: Turbulent mixing of two species whith or without chemical reactions, I&EC Fundamentals, 8(4), 655–659, 1969.

Valentini, R., Greco, S., Seufert, G., Bertin, N., Ciccioli, P., Cucinato, A., Brancaleoni, E., and Frattoni, M.: Fluxes of biogenic VOC from Mediterranean vegetation by trap enrichment relaxed eddy accumulation, Atmos. Environ., 31(SI), 229–238, 1997.

van Mieghem, J.: Les equations générales de la mécanique et de l'énergétique des milieux turbulents en vue des applications a la météorology, Inst. R. Météor. Belgique, Mém. XXXIV, 60 pp., 1949.

van Mieghem, J.: Atmospheric Energetics, Clarendon Press, Oxford, 306 pp., 1973.

Verver, G. H. L., van Dop, H., and Holtslag, A. A. M.: Turbulent mixing and the chemical breakdown of isoprene in the atmospheric boundary layer, J. Geophys. Res., 105(D3), 3983–4002, 2000.

Vila-Guerau de Arellano, J., Duynkerke, P. G., Jonker, P. J., and Builtjes, P. J. H.: An observational study on the effects of time and space averaging in photochemical models, Atmos. Environ., 27, 353–362, 1993.

Vila-Guerau de Arellano, J., Duynkerke, P. G., and Zeller, K. F.: Atmospheric surface layer similarity theory applied to chemical reactive species, J. Geophys. Res, 100(D1), 1397–1408, 1995.

Vinuesa, J.-F. and Vila-Guerau de Arellano, J.: Introducing effective reaction rates to account for the inefficient mixing of the convective boundary layer, Atmos. Environ., 39, 445–461, 2005.

Wahrhaft, Z.: Passive scalars in turbulent flows, Annu. Rev. Fluid Mech., 32, 203–240, 2000.

Wesely, M. L. and Hicks, B. B.: A review of the current status of knowledge on dry deposition. Atmos. Environ., 34, 2261–2282, 2000.

Zelger, M., Schween, J., Reuder, J., Gori, T., Simmerl, K., and Dlugi, R.: Turbulent transport, characteristic length and time scales above and within the BEMA forest site at Castelporziano, Atmos. Environ., 31(SI), 217–227, 1997.